

Bayesian Safe Policy Learning with Chance Constrained Optimization: Application to Military Security Assessment during the Vietnam War*

Zeyang Jia[†]Eli Ben-Michael[‡]Kosuke Imai[§]

May 28, 2024

Abstract

Algorithmic decisions and recommendations are used in many high-stakes decision-making settings such as criminal justice, medicine, and public policy. We investigate whether it would have been possible to improve a security assessment algorithm employed during the Vietnam War, using outcomes measured immediately after its introduction in late 1969. This empirical application raises several methodological challenges that frequently arise in high-stakes algorithmic decision-making. First, before implementing a new algorithm, it is essential to characterize and control the risk of yielding worse outcomes than the existing algorithm. Second, the existing algorithm is deterministic, and learning a new algorithm requires transparent extrapolation. Third, the existing algorithm involves discrete decision tables that are difficult to optimize over.

To address these challenges, we introduce the Average Conditional Risk (ACRisk), which first quantifies the risk that a new algorithmic policy leads to worse outcomes for subgroups of individual units and then averages this risk over the distribution of subgroups. We also propose a Bayesian policy learning framework that maximizes the posterior expected value while controlling the posterior expected ACRisk. This framework separates the estimation of heterogeneous treatment effects from policy optimization, enabling flexible estimation of effects and optimization over complex policy classes. We characterize the resulting chance-constrained optimization problem as a constrained linear programming problem. Our analysis shows that compared to the actual algorithm used during the Vietnam War, the learned algorithm assesses most regions as more secure and emphasizes economic and political factors over military factors.

Keywords: algorithmic decisions, Bayesian nonparametrics, conditional average treatment effect, decision tables, risk

*We acknowledge the partial support from Cisco Systems, Inc. (CG# 2370386), National Science Foundation (SES-2051196), and Sloan Foundation (Economics Program; 2020-13946).

[†]Ph.D. Student, Department of Statistics, Harvard University. 1 Oxford Street, Cambridge MA 02138. Email: zeyangjia@fas.harvard.edu

[‡]Assistant Professor, Department of Statistics & Data Science and Heinz College of Information Systems & Public Policy, Carnegie Mellon University. 4800 Forbes Avenue, Hamburg Hall, Pittsburgh PA 15213. Email: ebenmichael@cmu.edu URL: ebenmichael.github.io

[§]Professor, Department of Government and Department of Statistics, Harvard University. 1737 Cambridge Street, Institute for Quantitative Social Science, Cambridge MA 02138. Email: imai@harvard.edu URL: <https://imai.fas.harvard.edu>

1 Introduction

Algorithmic decisions and recommendations have long been used in areas as diverse as credit markets (Lauer, 2017) and war (Daddis, 2012). They are now increasingly integral to many aspects of today’s society, including online advertising (e.g., Li et al., 2010; Tang et al., 2013; Schwartz et al., 2017), medicine (e.g., Kamath et al., 2001; Nahum-Shani et al., 2018), and criminal justice (e.g., Imai et al., 2023; Greiner et al., 2020). A primary challenge when applying data-driven policies to consequential decision-making is to characterize and control the risk associated with any new policies learned from the data. Stakeholders in fields such as medicine, public policy, and the military may be concerned that the adoption of new data-derived policies could inadvertently lead to worse outcomes for some individuals in certain settings.

In this paper, we consider a particularly high-stakes setting, analyzing a United States (US) military security assessment policy that saw active use in the Vietnam War. During the war, the US military developed a data-driven scoring system called the Hamlet Evaluation System (HES) to produce a security score for each region (PACAF, 1969); commanders used these scores to make air strike decisions. A recent analysis based on a regression discontinuity design shows that the airstrikes had significantly negative effects on development outcomes including regional safety, economic, and civic society measures, and so were broadly counter-productive (Dell and Querubin, 2018).

We consider whether it would have been possible to improve the HES using contemporaneous data collected by the US military and related agencies to optimize for various development outcomes, while practically controlling the risk of worsening these outcomes in too many regions. In particular, the original HES was composed of various “sub-model scores” that measured different aspects of each region (e.g., economic variables, local administration, enemy military presence) based on survey responses. It then combined these into a single security score through a three-level hierarchical aggregation using pre-defined decision tables. The security scores were presented to Air Force commanders, who used them to make targeting decisions.

We focus on modifying these underlying decision tables while maintaining the transparency and interpretability of the original HES. Even though the system was in use over a half-century ago, this analysis serves three purposes. First, we show how to address methodological problems that are also common in other algorithmic decisions and recommendations. Second, because we limit to using data that were available at the time, our analysis serves as a case study on the development of optimal algorithm-assisted decision-making tools in high-stakes settings. Lastly, investigating the potential improvement gives insight into ways, in which the HES fell short, providing a historical lesson.

This empirical analysis poses several methodological challenges that are commonly encountered in high-stakes data-driven decision-making settings. First, we want to characterize and control the risk that a new learned decision, classification, or recommendation policy may lead to worse outcomes for some regions. Second, the HES is a deterministic function of the input data, implying that extrapolation

is necessary to learn new policies. Third, the security score is produced via a series of aggregations using decision tables, which is discrete and difficult to optimize over. Indeed, such decision tables are widely used in many public policy and medical decision-making settings (e.g., risk scores in the US criminal justice system [Greiner et al., 2020](#); [Imai et al., 2023](#)).

To address these challenges, we introduce a risk measure, the Average Conditional Risk (ACRisk), that first quantifies the risk of a given policy for groups of individual units with a specified set of covariates and then averages this conditional risk over the distribution of the covariates. In contrast to existing risk measures that characterize the uncertainty around the average performance of the policy (e.g., [Delage and Mannor, 2010](#); [Vakili and Zhao, 2015](#); [Bai et al., 2022](#)), the ACRisk measures the extent to which a learned policy negatively affects subgroups. This allows us to better characterize the potential heterogeneous risks of applying a new policy. With this risk measure in hand, we propose a Bayesian safe policy learning framework that maximizes the posterior expected value given the observed data while controlling the posterior expected ACRisk. We formulate this as a chance-constrained optimization problem and show how to convert it into a linear constraint, which can be solved as a standard optimization problem.

The primary advantages of the proposed framework are its flexibility and practical applicability. Because the chance-constrained optimization problem only relies on posterior samples, one can use popular Bayesian nonparametric regression models such as BART and Gaussian Process regression ([Rasmussen and Williams, 2006](#); [Chipman et al., 2010](#)), while efficiently finding an optimal policy within a complex policy class. This is especially helpful in settings such as ours with limited or no covariate overlap, where our framework allows for flexible extrapolation through the Bayesian prior. In contrast, frequentist notions of safe policy learning rely on robust optimization and require solving a minimax optimization problem over both the class of potential models and the class of potential policies, making it difficult to consider nonparametric models and complex policy classes at the same time ([Pu and Zhang, 2020](#); [Kallus and Zhou, 2021](#); [Ben-Michael et al., 2024](#); [Zhang et al., 2022](#)).

We show through simulation studies that controlling the posterior expected ACRisk effectively limits the ACRisk across various scenarios, reducing the risk of harming certain subgroups of units. We also find that although the proposed methodology is designed to be conservative, under some settings with a low signal-to-noise ratio, it yields a new policy whose average value is higher than a policy learned without the safety constraint. This is evidence that the proposed safety constraint can effectively regularize the policy optimization problem.

We apply the proposed methodology to find adaptations to the HES that lead to better outcomes — as measured by military, economic, and social objectives — while limiting the posterior probability that some regions experience worse outcomes under the new system than under the original HES. We consider two policy learning problems — one where we only change the last layer of the hierarchical aggregation that combines military, political and social economic sub-model scores, and another where we modify all of the decision tables used in the three-level hierarchical aggregation at the same time.

To deal with the latter complex case, we develop a stochastic optimization algorithm, based on random walks on partitions of directed acyclic graphs, that is generally applicable to decision tables.

Our analysis consistently shows that the original HES is too pessimistic—assessing regions as too insecure—and places too much emphasis on military factors. In contrast, our data-derived adaptations to the HES assess regions as more secure and rely more on economic and social factors to produce regional security scores.

Related literature. Recent years have witnessed a growing interest among statisticians and machine learning researchers in finding optimal policies from randomized experiments and observational studies (e.g. [Beygelzimer and Langford, 2009](#); [Qian and Murphy, 2011](#); [Dudík et al., 2011](#); [Zhao et al., 2012](#); [Zhang et al., 2012](#); [Swaminathan and Joachims, 2015](#); [Luedtke and Van Der Laan, 2016](#); [Zhou et al., 2017](#); [Kitagawa and Tetenov, 2018](#); [Kallus, 2018](#); [Athey and Wager, 2021](#); [Zhou et al., 2022](#)). These works typically consider the following two steps under a frequentist framework — first characterize the average performance, or value, of a given policy via the CATE, and then learn an optimal policy by maximizing the estimated value based on the observed data.

In contrast, we adopt a Bayesian perspective — first obtain the posterior distribution of the CATE given the observed data, and then learn an optimal policy by maximizing the posterior expected value. Bayesian methods have been widely used for causal inference (see [Li et al., 2022b](#), for a recent review). In particular, BART and Gaussian processes are often used to flexibly estimate the CATE ([Hill, 2011](#); [Branson et al., 2019](#); [Taddy et al., 2016](#); [Hahn et al., 2020](#)). However, it appears that the Bayesian approach has been rarely applied to policy learning ([Kasy, 2018](#)). Our proposed framework takes advantage of these popular Bayesian nonparametric methods for safe policy learning.

There is also a growing literature on policy learning in scenarios where the CATE is unidentifiable ([Manski, 2007](#); [Pu and Zhang, 2020](#); [Yata, 2021](#); [Kallus and Zhou, 2021](#); [Ben-Michael et al., 2021](#); [Zhang et al., 2022](#); [Ben-Michael et al., 2024](#)). These include observational studies with unmeasured confounders ([Kallus and Zhou, 2021](#)), studies with noncompliance or an instrumental variable ([Pu and Zhang, 2020](#)), studies that lack overlap due to deterministic treatment rules ([Ben-Michael et al., 2021](#); [Zhang et al., 2022](#)), and utility functions that involve the joint set of potential outcomes ([Ben-Michael et al., 2024](#)). These works first partially identify the value of a given policy then find the policy that maximizes the worst-case value using robust optimization. Our approach differs in that we decouple estimation and policy optimization by only relying on posterior samples for policy learning.

In the Reinforcement Learning (RL) literature, various notions of safety have been studied (e.g., safe reinforcement learning, risk averse reinforcement learning, pessimistic reinforcement learning; see [Garcia and Fernández \(2015\)](#)). For example, [Geibel and Wyszotzki \(2005\)](#) control the risk of the agent visiting a “dangerous state” by explicitly imposing a risk constraint when finding an optimal policy. In contrast, [Sato et al. \(2001\)](#) and [Vakili and Zhao \(2015\)](#) use the variance of the return as a penalty term in the objective when finding an optimal policy with a high expected return and low variance.

While this RL literature focuses on online settings where the algorithm is designed to avoid risks during exploration, we study the risk of applying data-driven policies in offline settings.

We also extend existing work by developing the notion of ACRisk and using it as a constraint in optimizing the posterior expected value of a new policy. A related literature is *pessimistic offline RL*, which quantifies the risk of a given policy using the lower confidence bound (LCB) of the value, and finds a policy that has the best LCB (Jin et al., 2021; Buckman et al., 2020; Zanette et al., 2021; Xie et al., 2021; Chen and Jiang, 2022; Rashidinejad et al., 2021; Yin and Wang, 2021; Shi et al., 2022; Yan et al., 2022; Uehara and Sun, 2021; Bai et al., 2022; Jin et al., 2022). In contrast, the proposed ACRisk measures the extent to which a new policy negatively affects some groups of individuals when compared to the baseline policy.

Finally, our work is also related to chance constrained optimization, which is widely used in the analysis of decision making under uncertainty (e.g., Schwarm and Nikolaou, 1999; Filar et al., 1995; Delage and Mannor, 2007, 2010; Farina et al., 2016). For example, Delage and Mannor (2010) consider chance constrained control for Markov Decision Processes. They assume a Gaussian model for the reward distribution and use chance constrained optimization to find a policy that achieves low regret with high posterior probability. In contrast, our method considers a more general setup beyond the Gaussian model and uses the posterior expected value of the ACRisk as a constraint.

Outline of the paper. The remainder of this paper is organized as follows. Section 2 describes U.S. military security assessment in the Vietnam War, the HES, and the related empirical policy learning problem. Section 3 introduces a formal setup, and Section 4 describes the Bayesian safe policy learning framework and the chance-constrained optimization procedure, as well as implementation via Gaussian Processes and Bayesian Causal Forests. Section 5 presents numerical experiments evaluating our proposal. Section 6 applies the Bayesian safe policy learning method to the Military security assessment problem. Section 7 concludes and discusses limitations and future directions.

2 Military Security Assessment during the Vietnam War

During the Vietnam War, the United States Air Force (USAF) conducted numerous air strike campaigns. One factor guiding USAF commanders in making targeting decisions was a data-driven scoring system called the Hamlet Evaluation System (HES) whose goal was to provide a metric for regional security based on survey data (PACAF, 1969). We briefly describe the HES and its aggregation rules, as well as the policy learning problem we consider. Specifically, we focus on the second version of the HES, which was developed in 1969 and was originally analyzed by Dell and Querubin (2018).

2.1 The Hamlet Evaluation System

The HES was based on a total of 169 military, political, and socioeconomic indicators collected quarterly by Civil Operations and Revolutionary Development Support (CORDS), a joint civilian-military agency.

These indicators were then categorized and summarized as 20 continuous “sub-model” scores.¹ Each sub-model score ranges from 1 to 5 and measures a different aspect of a given region, such as *Enemy Military Activity*, *Economic Activity*, and *Public Health*. The HES aggregates these 20 continuous-valued sub-model scores into a single integer-valued security score ranging between 1 and 5. The sub-model scores are all semantically ordered so that lower values indicate that a region is “worse” in the metric. The final HES score is ordered so that regions with a score of 1 should get the highest priority from USAF commanders and those with a score of 5 should get the lowest. After calculating the security score for each region at the beginning of a quarter, USAF commanders used these scores to make air strike decisions during that quarter.

Although several other factors contributed to the determination of eventual air strike targets, [Dell and Querubin \(2018\)](#) show that regions which fell just above a security score threshold — and hence had a higher security score — were less likely to be subject to air strikes than those regions just below the threshold. Using a regression discontinuity design, the authors find that the air strike campaign was largely counter-productive, increasing insurgency activities and decreasing civic engagements.

Given this finding, we investigate whether it is possible to improve the original HES security evaluation with the contemporaneous data available during the war. We focus on the first quarter of the HES deployment (Q4 1969) and use the military impact assessments taken at the beginning of the succeeding quarter (January 1970) as the outcome to measure the efficacy of the HES.

2.2 Aggregation via Decision Tables

The HES aggregates 20 continuous sub-model scores to a single integer-valued security score that take a value in $\{1, 2, 3, 4, 5\}$, as shown in Figure 1. This hierarchical aggregation process starts by rounding the 20 continuous sub-model scores to the nearest integer in $\{1, 2, 3, 4, 5\}$. The security score then is produced through the following three steps. First, 18 out of these 20 rounded sub-model scores are aggregated to six integer-valued model scores relating to Enemy Military, Friendly Military, Enemy Political, Government Political, Social, and Economic model scores. Second, the resulting six model scores, along with two remaining inputs (impact of military activity and political mobilization), are aggregated to three higher tier integer-valued scores — Military, Political, and Social Economic model scores. Finally, these three scores are further aggregated to the integer-valued single security score.

At each step of aggregation, the HES uses a two-way or three-way decision table indicated by the number shown in each circle of Figure 1. These tables take two or three integer-valued scores, ranging from 1 to 5, and return a new score, which takes a value in $\{1, 2, 3, 4, 5\}$. Figures ?? and ?? in the appendix show the two-way and three-way decision tables used in the HES, respectively. For example, the two-way decision table maps an input of $(2, 3)$ to an output of 2. In the HES, the same two-way and three-way tables are used across all levels of aggregation.

¹The HES actually produces 19 different sub-model scores from the 169 indicators, but one sub-model score is used twice in the later aggregation. For simplicity and clarity, consider these to be 20 scores.

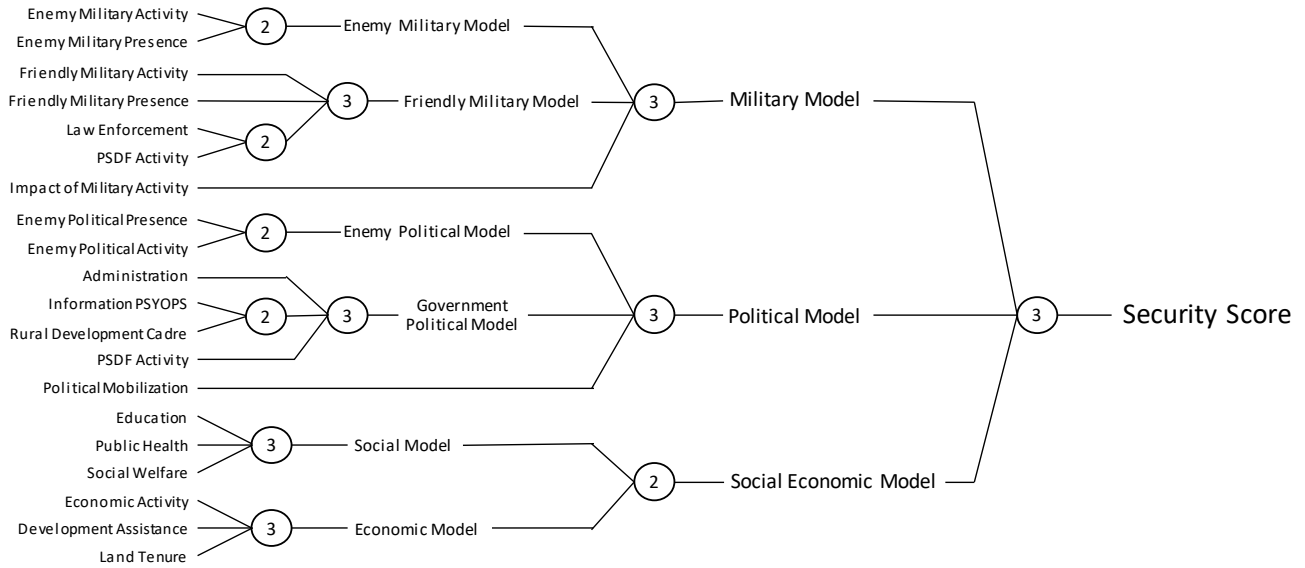


Figure 1: Aggregation of 20 sub-model scores. The Hamlet Evaluation System (HES) uses 20 sub-model scores as inputs, and aggregates them using two-way and three-way decision tables. Each circle corresponds to one aggregation based on the two-way or three-way decision table, and the decision tables used in different circles are the same.

In our analysis, we modify the underlying two-way and three-way decision tables. We do not modify the hierarchical structure itself or using black-box machine learning tools, because the hierarchical structure contains substantial domain knowledge, and we wish to retain the transparency of the original system. This also facilitates easier comparisons between our data-derived modifications and the original HES system. As we discuss and explore in Section 6.3, altering the underlying decision tables alters the implicit influence of each of the 20 factors in constructing the overall HES score. We note, however, that our methodological development in the next sections can also be used to adjust the hierarchy itself or to use black box methods, although there may be additional computational considerations.

2.3 Evidence-based Policy Learning

To measure the impact of air strikes and learn a new decision policy, we analyze three binary outcomes that reflect regional security, economy, and civic society. These outcomes are based on survey responses from multiple sources collected in January 1970, after the period of air strikes in the final quarter of 1969 (Dell and Querubin, 2018). During this period, USAF commanders targeted 1024 of the 1954 regions defined by the HES.² Our objective is to develop a new decision rule that generates appropriate security scores based on the 20 continuous sub-model scores. It is worth noting that our decision variable is the output security score from the HES rather than the air strike decision itself, which is made by commanders. We aim to optimize the way, in which the final security score is produced from the 20 sub-model scores to achieve the best overall outcomes in regional security, economy, and

²See Appendix Table ?? and Figure ?? for other summary statistics as well as the average values of the security score and various sub-model scores

civic society (marginalizing over commanders’ airstrike decisions).

This application yields several methodological challenges. First, the stakes of this decision are high and there is potential heterogeneity across regions. This motivates a safe policy learning approach that limits the possibility of generating worse outcomes under a new, learned policy for some regions than under the existing policy. Second, the existing policy is deterministic, rather than stochastic. Therefore, due to the lack of overlap between regions that received different HES scores, we must extrapolate when estimating the potential outcomes under a new policy. Lastly, the existing policy is based on multiple decision tables. Thus, to keep the existing structure of the policy, we must solve a complex optimization problem. We now develop a new Bayesian safe policy framework that addresses these challenges.

3 Preliminaries

Before we develop our Bayesian policy learning framework, we describe the problem setup and notation. In addition, we provide a brief review of Bayesian policy learning.

3.1 Setup and Notation

We consider an individualized treatment rule or policy, which deterministically maps a set of p pre-treatment covariates $\mathbf{X} \in \mathcal{X} \subseteq \mathbb{R}^p$ to a multivalued decision $D \in \mathcal{D} = \{0, 1, \dots, K-1\}$ where K denotes the total number of decision categories. Formally, a policy is defined as a function $\delta : \mathcal{X} \rightarrow \mathcal{D}$. We have a simple random sample of n observations from the population of interest \mathcal{P} , which is characterized by the joint distribution of $\{\mathbf{X}, Y(0), Y(1), \dots, Y(K-1)\}$ where $Y(k)$ represents a potential outcome under decision $D = k$ with $k \in \mathcal{D}$ and the observed outcome is given by $Y_i = Y_i(D_i)$ (Neyman, 1923; Rubin, 1974). This notation implicitly assumes no interference between units (Rubin, 1980).

We also assume that the decision is unconfounded given the covariates, i.e., $\{Y_i(k)\}_{k=0}^{K-1} \perp\!\!\!\perp D_i \mid \mathbf{X}_i$ (Rosenbaum and Rubin, 1983). However, we do not assume that there exists covariate overlap for treated and controlled units — i.e., $0 < \Pr(D_i = k \mid \mathbf{X}_i = \mathbf{x}) < 1$ for all $k \in \mathcal{D}$ and $\mathbf{x} \in \mathcal{X}$. The lack of overlap is motivated by the fact that in many settings, the data are collected under an existing deterministic policy (Ben-Michael et al., 2021; Zhang et al., 2022).

Suppose that a policy-maker defines a utility function $u : \{0, 1, \dots, K-1\} \times \mathcal{Y} \rightarrow \mathbb{R}$, which maps every decision-outcome pair to a real-valued utility. Then, the expected utility or value of policy δ in a policy class Δ is given by,

$$V(\delta) := \mathbb{E}[u(\delta(\mathbf{X}), Y(\delta(\mathbf{X})))]. \quad (1)$$

Our goal is to find an optimal policy within a policy class Δ that has a high value relative to the existing policy $\tilde{\delta}$, which also belongs to the same policy class Δ (Ben-Michael et al., 2021; Wei et al., 2022). In our application, the baseline policy is a deterministic rule that produces the security score in the HES. Our goal is to derive a new policy whose average value is higher than that of the original policy subject to a safety constraint that will be introduced in Section 4.

3.2 Bayesian Policy Learning

We next briefly introduce the basic elements of Bayesian policy learning (see [Ding and Li, 2018](#); [Li et al., 2022b](#), for reviews of Bayesian causal inference). Under the Bayesian framework, all parameters are regarded as random variables. Following the convention, we will use upper and lower case characters to represent parameters and their realizations, respectively.

Suppose that the marginal distribution of potential outcomes is characterized by a possibly infinite dimensional parameter Θ . Bayesian policy learning proceeds in two steps. First, we specify a prior distribution $\pi(\Theta)$ on the parameter Θ and compute its posterior distribution using Bayes' rule,

$$\pi(\Theta \mid \{\mathbf{X}_i, D_i, Y_i\}_{i=1}^n) \propto \prod_{i=1}^n p(Y_i \mid \Theta, \mathbf{X}_i, D_i) \pi(\Theta). \quad (2)$$

Under Bayesian policy learning, given the posterior distribution of Θ , the optimal policy maximizes the posterior expected value,

$$\delta_{opt} = \operatorname{argmax}_{\delta \in \Delta} \mathbb{E}[V(\delta; \Theta) \mid \{D_i, \mathbf{X}_i, Y_i\}_{i=1}^n], \quad (3)$$

where $V(\delta; \Theta) := \mathbb{E}[u(\delta(\mathbf{X}), Y(\delta(\mathbf{X}))) \mid \Theta]$. We explicitly use the notation $V(\delta; \Theta)$ to emphasize its dependence on the parameter Θ as well as the policy δ . Specifically, $V(\delta; \Theta)$ averages over both the marginal distribution of \mathbf{X} , and the conditional distribution of $Y(\delta(\mathbf{X}))$ given \mathbf{X} and Θ . The expectation in Equation (3) is taken over the posterior distribution of Θ given the observed data.

To solve the optimization problem in Equation (3), we can rewrite the expectation over parameter Θ , covariates \mathbf{X} , and potential outcome $Y(\delta(\mathbf{X}))$ as,

$$\mathbb{E}[V(\delta; \Theta) \mid \{\mathbf{X}_i, D_i, Y_i\}_{i=1}^n] = \int_{\mathcal{X}} \sum_{d=0}^{K-1} \mathbb{E}[u(d, Y(d)) \mid \mathbf{X} = \mathbf{x}, \{\mathbf{X}_i, D_i, Y_i\}_{i=1}^n] \mathbb{I}(\delta(\mathbf{x}) = d) dF(\mathbf{x}), \quad (4)$$

where the inside expectation is taken over the posterior distribution of Θ given the observed data, and the distribution of the potential outcomes given Θ and \mathbf{X} . The outside expectation is taken over the distribution of \mathbf{X} , where F is the CDF of \mathbf{X} . For simplicity, we will assume the distribution of X in the target population is known.

Thus, the original problem in Equation (3) can consist of two steps: (i) estimate the posterior expected utility of decision d given a covariate profile \mathbf{x} , $\mathbb{E}[u(d, Y(d)) \mid \mathbf{X} = \mathbf{x}, \{\mathbf{X}_i, D_i, Y_i\}_{i=1}^n]$, and (ii) find the optimal policy δ by solving the optimization (4) with the estimated values. This formulation separates the problem of computing the posterior distribution from that of finding an optimal policy.

4 The Proposed Methodology

We now describe our Bayesian safe policy learning framework. We begin by introducing a new risk metric, the Average Conditional Risk (ACRisk), that represents the probability that a new policy

yields a worse expected utility conditional on covariates than the baseline policy. We then propose to maximize the posterior expected value of the new policy while limiting the posterior expected ACRisk. Our methodology consists of two steps: first estimating the conditional average treatment effect (CATE) using a flexible Bayesian model, and then finding a policy within the policy class that maximizes the posterior expected value while controlling the posterior expected ACRisk. Finally, we show that this chance-constrained optimization problem can be written as a standard Bayesian policy learning problem with linear constraints, avoiding additional computational complexity.

4.1 Average Conditional Risk (ACRisk)

In the existing literature, the risk of a policy is typically measured through uncertainty about its value. We then seek a policy that has a high value with a small estimation uncertainty. One limitation of this common approach is its failure to account for potential heterogeneity in risk across different groups of individuals. A policy that performs well on average may not benefit everyone. In our empirical application, a security assessment rule that is effective on average may negatively impact some regions. While the risk due to estimation uncertainty will become small as the sample size increases, this inherent risk due to heterogeneous treatment effects will remain, even in large samples.

To address this, we introduce a new risk measure, the Average Conditional Risk (ACRisk), which represents the probability that, conditional on the covariates, a policy yields a worse expected utility than the baseline policy.

Definition 1 (Average Conditional Risk (ACRisk)). For a given policy δ , the Average Conditional Risk with respect to a baseline policy $\tilde{\delta}$ is

$$R(\delta, \tilde{\delta}; \boldsymbol{\theta}) := \mathbb{P} \left(\mathbb{E} \left[u(\delta(\mathbf{X}), Y(\delta(\mathbf{X}))) \mid \mathbf{X}, \boldsymbol{\Theta} = \boldsymbol{\theta} \right] < \mathbb{E} \left[u(\tilde{\delta}(\mathbf{X}), Y(\tilde{\delta}(\mathbf{X}))) \mid \mathbf{X}, \boldsymbol{\Theta} = \boldsymbol{\theta} \right] \right),$$

where $\boldsymbol{\Theta}$ represents the possibly infinite-dimensional parameter that governs the marginal distributions of potential outcomes.

The inner expectation in the above definition is taken over the conditional distribution of $Y(\delta(\mathbf{X}))$ given \mathbf{X} and $\boldsymbol{\Theta}$ while the outer probability is defined with respect to the marginal distribution of \mathbf{X} . We use the above notation to make it explicit that the ACRisk depends on the parameter $\boldsymbol{\Theta}$, which governs the conditional distribution of potential outcomes given the covariates \mathbf{X} . Note that under this definition, $R(\tilde{\delta}, \tilde{\delta}; \boldsymbol{\theta}) = 0$ for any value of $\boldsymbol{\theta}$.

The ACRisk first evaluates whether a group of individuals with a certain set of covariates has a lower expected utility under policy δ than under the baseline policy $\tilde{\delta}$. It then computes the proportion of such at-risk groups in the population by averaging over the distribution of covariates. The ACRisk is dependent on the covariates we choose, and using different set of covariates can result in different at-risk groups, potentially leading to different ACRisk values.

Table 1 provides a numerical example where both Policies I and II outperform the baseline policy. While the improvement of Policy I comes at the expense of group B, Policy II performs equally well for both groups. As a result, the ACRisk of Policy I is higher with 50% of the population at risk.

	Conditional expected utility		Value	ACRisk
	Group A (50%)	Group B (50%)		
Baseline policy	0	0	0	0
Policy I	4	-2	1	0.5
Policy II	1	1	1	0

Table 1: A numerical example that illustrates the Average Conditional Risk (ACRisk). In this example, both Policies I and II outperform the baseline policy on average, but the improvement of Policy I comes at the expense of the group B. The ACRisk shows that 50% of the population, which is the size of the group B in this example, is at risk.

We note that the ACRisk is a risk measure based on groups (defined by covariates \mathbf{X}). In particular, the ACRisk differs from the following individual measure of risk.

Definition 2 (Average Individual Risk (AIRisk)). For a given policy δ , its average individual risk with respect to a baseline policy $\tilde{\delta}$ is defined as,

$$R^*(\delta, \tilde{\delta}; \lambda) := \mathbb{P}\left(u(\delta(\mathbf{X}), Y(\delta(\mathbf{X}))) < u(\delta(\mathbf{X}), Y(\tilde{\delta}(\mathbf{X}))) \mid \Lambda = \lambda\right),$$

where Λ represents a (possibly infinite dimensional) parameter that governs the joint distribution of potential outcomes.

Unlike the ACRisk, the AIRisk is not identifiable because it depends on the joint distribution of potential outcomes. One possible strategy is to control an upper bound of the AIRisk (Kallus, 2022; Ben-Michael et al., 2024; Li et al., 2022a). We leave the development of safe policy learning in terms of the AIRisk to future research and focus on the ACRisk for the remainder of this paper.

To control the ACRisk, we must estimate the parameter Θ . Under our Bayesian safe policy learning framework, we consider the posterior average of the ACRisk, which we call the Posterior Average Conditional Risk or PACRisk. This measure allows us to directly incorporate estimation uncertainty into our analysis.

Definition 3 (Posterior Average Conditional Risk (PACRisk)). For a given policy δ , the Posterior Average Conditional Risk with respect to a baseline policy $\tilde{\delta}$ is

$$R_p(\delta, \tilde{\delta}) := \mathbb{E}\left[R(\delta, \tilde{\delta}; \Theta) \mid \{\mathbf{X}_i, D_i, Y_i\}_{i=1}^n\right],$$

where the expectation is taken over the posterior distribution of Θ given the observed data $\{\mathbf{X}_i, D_i, Y_i\}_{i=1}^n$.

4.2 Bayesian Safe Policy Learning with Chance Constrained Optimization

We now propose a Bayesian safe policy learning procedure that limits the PACRisk introduced above (Definition 3). Specifically, we find a policy within a policy class Δ that maximizes the posterior average value while limiting the PACRisk below a specified threshold $\epsilon \in [0, 1]$,

$$\begin{aligned} \delta_{\text{safe}} &= \underset{\delta \in \Delta}{\operatorname{argmax}} \mathbb{E}[V(\delta; \Theta) \mid \{\mathbf{X}_i, D_i, Y_i\}_{i=1}^n] \\ &\text{subject to } \mathbb{E}\left[R(\delta, \tilde{\delta}; \Theta) \mid \{\mathbf{X}_i, D_i, Y_i\}_{i=1}^n\right] \leq \epsilon, \end{aligned} \tag{5}$$

The expectation in the optimization target is taken over the posterior distribution of the parameter Θ . We typically choose a policy class Δ that contains the baseline policy so that a solution to Equation (5) always exists. The constraint in Equation (5) ensures that for a randomly selected group of individuals, δ_{safe} has an at most ϵ posterior probability of yielding a worse expected value for the group than the baseline policy $\tilde{\delta}$. Thus, a smaller value of ϵ yields a safer policy that is more conservative, limiting the extent of changes to the baseline policy.

A standard Bayesian policy maximizes the posterior expected utility, modifying the baseline policy for subgroups where the posterior expected CATE is large. However, the additional PACRisk constraint in Equation (4) prioritizes changes to the baseline policy for those subgroups whose posterior expected value of the CATE is large and its posterior uncertainty is small. Consider a toy example, in which \mathbf{X} is a binary variable and $\Theta = (\theta_0, \theta_1)$ where θ_0 and θ_1 are the CATEs for $\mathbf{X} = 0$ and $\mathbf{X} = 1$, respectively. The baseline policy is to treat nobody. In addition, suppose that the posterior distributions of θ_0 and θ_1 are $N(10, 100)$ and $N(1, 0.1)$, respectively. Under this setting, the Bayesian optimal policy δ_{opt} will treat everyone even though the treatment effect for the subgroup $\mathbf{X} = 0$ is highly uncertain. In contrast, the PACRisk constraint in our methodology considers the posterior probability of the group-level positive treatment effect, and will be more conservative when changing the baseline policy may negatively affect some subgroups due to a high degree of posterior uncertainty of the CATE.

One potential drawback of chance constraints such as the one shown in Equation (5) is its computational difficulty due to their complex dependency on both the parameter Θ and the policy δ . This makes it challenging to determine how the value of the constraint changes as a function of the policy δ . For this reason, researchers typically impose strong assumptions on the marginal distribution of potential outcomes and the parameter Θ to obtain a closed-form solution instead (e.g., [Delage and Mannor, 2010](#); [Vitus et al., 2015](#); [Mowbray et al., 2022](#)).

We overcome this challenge by formulating Equation (5) as a deterministic optimization problem with a linear constraint that separates the estimation of CATE from policy optimization in the manner similar to Equation (4) under the standard Bayesian policy learning. The following theorem formally establishes the equivalence between the chance constraint optimization in Equation (5) and a constrained linear programming problem.

Theorem 1 (Control of the PACRisk as a Linear Constraint). Define the posterior conditional benefit and risk of decision k relative to the existing policy $\tilde{\delta}$ as,

$$b_k(\mathbf{x}) := \mathbb{E}[\tau_k(\mathbf{x}, \Theta) \mid \{D_i, \mathbf{X}_i, Y_i\}_{i=1}^n], \quad r_k(\mathbf{x}) := \mathbb{P}(\tau_k(\mathbf{x}, \Theta) < 0 \mid \{D_i, \mathbf{X}_i, Y_i\}_{i=1}^n),$$

where $\tau_k(\mathbf{x}, \theta) := \mathbb{E}[u(k, Y(k)) - u(\tilde{\delta}(\mathbf{x}), Y(\tilde{\delta}(\mathbf{x}))) \mid \mathbf{X} = \mathbf{x}, \Theta = \theta]$. Then, the chance-constrained

Algorithm 1: Bayesian Safe Policy Learning based on Posterior Draws

Input: Data $\{\mathbf{X}_i, D_i, Y_i\}_{i=1}^n$; A total of M posterior draws, i.e., $\{\Theta^{(m)}\}_{m=1}^M$; Covariate distribution function $F(x)$

Output: Bayesian safe policy $\hat{\delta}_{\text{safe}} : \mathcal{X} \rightarrow \mathcal{D} = \{0, 1, \dots, K-1\}$

- 1 Approximate the posterior conditional benefit of decision k ,
 $b_k(\mathbf{x}) = \mathbb{E}[\tau_k(\mathbf{x}, \Theta) \mid \{\mathbf{X}_i, D_i, Y_i\}_{i=1}^n]$, by the sample average of posterior draws for $\mathbf{x} \in \mathcal{X}$:

$$\hat{b}_k(\mathbf{x}) = \frac{1}{M} \sum_{m=1}^M \tau_k(\mathbf{x}, \Theta^{(m)})$$

- 2 Approximate the posterior conditional risk of decision k .
 $r_k(\mathbf{x}) = \mathbb{P}(\tau_k(\mathbf{x}, \Theta) < 0 \mid \{D_i, \mathbf{X}_i, Y_i\}_{i=1}^n)$, by the sample average of posterior draws for $\mathbf{x} \in \mathcal{X}$:

$$\hat{r}_k(\mathbf{x}) = \frac{1}{M} \sum_{m=1}^M I\{\tau_k(\mathbf{x}, \Theta^{(m)}) < 0\}$$

- 3 Solve this approximated optimization problem:

$$\begin{aligned} \hat{\delta}_{\text{safe}} = \operatorname{argmax}_{\delta \in \Delta} & \sum_{k=0}^{K-1} \int I(\delta(\mathbf{X}) = k) \hat{b}_k(\mathbf{X}) dF(\mathbf{X}) \\ \text{subject to} & \sum_{k=0}^{K-1} \int I(\delta(\mathbf{X}) = k) \hat{r}_k(\mathbf{x}) dF(\mathbf{X}) \leq \epsilon \end{aligned}$$

optimization defined in Equation (5) is equivalent to the following deterministic optimization problem,

$$\begin{aligned} \delta_{\text{safe}} = \operatorname{argmax}_{\delta \in \Delta} & \sum_{k=0}^{K-1} \int I(\delta(\mathbf{X}) = k) b_k(\mathbf{X}) dF(\mathbf{X}) \\ \text{subject to} & \sum_{k=0}^{K-1} \int I(\delta(\mathbf{X}) = k) r_k(\mathbf{x}) dF(\mathbf{X}) \leq \epsilon \end{aligned} \tag{6}$$

where $F(\mathbf{x})$ is the cumulative distribution function of covariates \mathbf{X} .

Proof is given in Appendix ???. In the theorem, $\tau_k(x, \theta)$ is the improvement in the conditional expected utility when changing the decision $\tilde{\delta}(x)$ to k where $\{\tau_k(x, \Theta)\}_{k=0}^{K-1}$ is fully determined by $K-1$ pairwise CATEs between K decisions. In practice, we use the empirical CDF for $F(\mathbf{X})$.

Theorem 1 enables us to explicitly separate the posterior of Θ and the policy δ in the chance-constrained optimization. We note that this formulation is possible because the ACRisk of a policy δ is a weighted average of its conditional risk given \mathbf{X} , which can be represented by $\{r_k(\mathbf{x})\}_{k=0}^{K-1}$. We can first calculate the conditional improvement and risk, i.e., $b_k(\mathbf{x})$ and $r_k(\mathbf{x})$, using either closed-form calculation or samples from posterior draws. Then, like the standard Bayesian policy learning, we can solve the constrained policy optimization problem based on $b_k(\mathbf{x})$ and $r_k(\mathbf{x})$. Algorithm 1 summarizes the procedure of our proposed Bayesian safe policy learning based on the posterior draws of Θ .

4.3 Bayesian CATE estimation

A primary advantage of the proposed Bayesian safe policy learning framework introduced above is separating the tasks of estimating the CATE and optimizing the policy. This means that our framework can readily accommodate the use of flexible Bayesian nonparametric models for CATE estimation.

As an example that mirrors our empirical application, suppose that we have an ordered decision, $k \in \{0, 1, \dots, K - 1\}$ and a continuous outcome. We begin by modeling the marginal distribution of the baseline potential outcome $Y_i(0)$ and then the $K - 1$ CATEs between two adjacent treatment levels. Specifically, we assume the following model,

$$Y_i(k) = \sum_{d=0}^k f_d(X_i) + \epsilon_i, \quad \forall k \in \{0, 1, \dots, K - 1\}$$

where ϵ_i is an i.i.d Gaussian random variable with mean 0 and variance σ^2 , $f_0(\mathbf{x}) = \mathbb{E}[Y(0) | \mathbf{X} = \mathbf{x}]$, and $f_k(\mathbf{x}) = \mathbb{E}[Y(k) - Y(k - 1) | \mathbf{X} = \mathbf{x}]$ for $1 \leq k \leq K - 1$. Here, we have an infinite dimensional parameter $\Theta = \left(\sigma^2, \{f_k(\cdot)\}_{k=0}^{K-1}\right)$ that determines the marginal distribution of each potential outcome $Y(k)$ given covariates \mathbf{X} . If we have binary or categorical outcomes, we use a link function to transform the mean outcome to a continuous scale, e.g.,

$$Y_i(d) | \mathbf{X}_i \sim \text{Bernoulli}(p_d(\mathbf{X}_i)) \text{ where } p_d(\mathbf{X}_i) = g^{-1}\left(\sum_{k=1}^d f_{k-1}(\mathbf{X}_i)\right) \quad (7)$$

where $g^{-1}(\cdot)$ is the inverse link function.

In principle, any Bayesian method can be applied for modeling $\{f_k(\cdot)\}_{k=0}^{K-1}$. In the Appendix ??, we discussed two popular methods, Bayesian Additive Regression Trees (BART) and Gaussian Processes (GP) to demonstrate how such models can be accommodated.

5 A Simulation Study

In this section, we conduct a simulation study to examine the empirical performance of the proposed Bayesian safe policy learning methodology. To highlight the key concepts, we consider a simple setup with a binary decision.

5.1 Setup

We consider the following data generating processes with the number of observations n varying from 50 to 500, i.e., $n \in \{50, 100, 200, 500\}$. There are two covariates $\mathbf{X} = (X_1, X_2)$ that are independently and identically distributed according to a uniform distribution $X_1, X_2 \stackrel{i.i.d}{\sim} \text{Uniform}(-1, 1)$. There are two scenarios, one with covariate overlap and the other without it:

- **Scenario I (with covariate overlap):** The data are collected through a randomized experiment with $\mathbb{P}(D = 1 | \mathbf{X} = \mathbf{x}) = 0.5, \forall \mathbf{x} \in \mathcal{X}$. Here, the baseline policy is to treat nobody, i.e., $\tilde{\delta}(\mathbf{x}) =$

$0, \forall \mathbf{x} \in \mathcal{X}$.

- **Scenario II (without covariate overlap):** The data are collected under a deterministic policy $\tilde{\delta}(x) = I(x_1 > 0.5)$, which serves as the baseline policy. Thus, the treatment assignment is also deterministic, i.e., $\mathbb{P}(D = 1 \mid \mathbf{X} = \mathbf{x}) = \tilde{\delta}(\mathbf{x})$.

Within each simulation scenario, we specify the outcome model as,³

$$Y \mid \mathbf{X} \sim N(X_1 + X_2 + \{4I(X_1 > 0, X_2 > 0) - 2\}D|X_1||X_2|, \sigma^2)$$

where we consider a high signal-to-noise ratio case ($\sigma = 1$), a medium signal-to-noise ratio case ($\sigma = 2$), and a low signal-to-noise ratio case ($\sigma = 3$). In this setup, treatment is effective for individuals with $X_1 > 0, X_2 > 0$. Finally, we set the utility to be equal to the outcome, i.e., $u(d, y) = y$.

We consider policies based on a linear separation of the covariate space \mathcal{X} :

$$\Delta := \{\delta(\cdot, \cdot) : \delta(x_1, x_2) = I(ax_1 + bx_2 + c > 0); a, b, c \in \mathbb{R}\} \quad (8)$$

Notice that this policy class does not contain the oracle treatment rule — giving the treatment to individuals with $X_1 > 0$ and $X_2 > 0$. We apply the proposed Bayesian safe policy learning methods, and use the empirical distribution of the covariates \mathbf{X} as an approximate CDF of \mathbf{X} .

For Scenario I with covariate overlap, we use Bayesian Causal Forests (BCF) to estimate the CATE and the expected outcome under the control condition, i.e., $\mathbb{E}(Y(0))$, with the default hyperprior parameter specification suggested by [Hahn et al. \(2020\)](#). For modeling $\mathbb{E}[Y(0)|\mathbf{X}]$, we use 200 trees and hyperparameters of $\beta = 2, \eta = 0.95$. For modeling the CATE, we impose a stronger prior and use a BART model with 50 trees, and $\beta = 3, \eta = 0.25$. Here, β is the penalization hyperparameter for the depth of trees (larger values lead to more shallow trees) and η is the splitting probability hyperparameter (larger values lead to deeper trees).

For Scenario II without covariate overlap, we use Gaussian Process regression (GP) to model the expected outcome under the control condition as well as the CATE. We set the kernel of the Gaussian process as a Matern kernel with parameter $l = 0.5, 1$ or $2, \nu = 3/2$ (see Equation (??)). We use a non-informative prior where the mean function of the GP, $m(x)$, is set to 0. For other hyperparameters in the kernel function, we set the length scale to $\{0.5, 1, 2\}$ which correspond to a *non-smooth*, *moderately smooth*, and *highly smooth* CATE. We set σ_0^2 to $\{1, 4, 16\}$ which corresponds to a *strong*, *medium*, and *weak* prior.

For both methods, we use `Stan` ([Carpenter et al., 2017](#)) to compute 2,000 posterior samples from two chains with a burn-in period of 500 samples.

³We also consider a data generating process with binary outcomes in Appendix ???. The results are broadly similar to the continuous case.

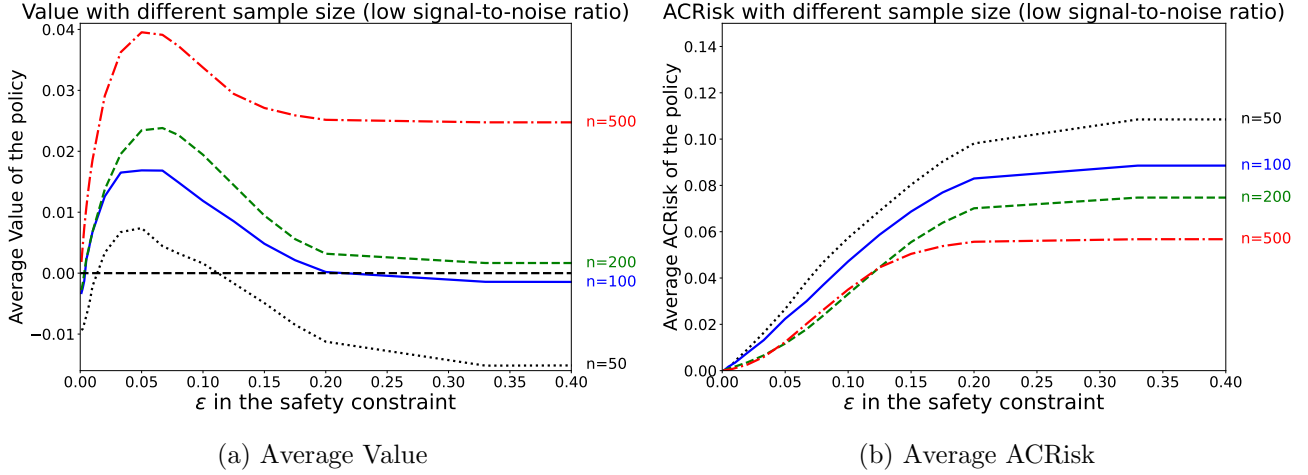


Figure 2: The average value (left panel) and ACRisk (right panel) of the learned policies using the data with covariate overlap, varying the safety constraint ϵ and sample size n .

5.2 Findings

Since we know the true data generating process, we can calculate the ACRisk for the learned policy under different policy learning setups. Since the proposed methodology controls the PACRisk, it is of interest to investigate how the ACRisk of the learned policy as well as the policy value change as functions of the safety constraint ϵ in Equation (5). We also examine the influence of the prior distribution on the performance of the proposed methodology when there is no covariate overlap.

Sample size and signal strength. Figure 2 presents the average value (left panel) and average ACRisk (right panel) of learned policies under different values of the safety constraint ϵ (x -axis) with various sample sizes, using the continuous outcome model. Similarly, Figure ?? in the appendix shows the results with different values of the safety constraint ϵ and signal-to-noise ratio. The data generating process follows Scenario I, and there is no extrapolation. As expected, we find that a weaker of safety constraint (i.e., a greater value of ϵ) leads to a greater ACRisk of the learned policy, reaching a plateau that corresponds to the ACRisk obtained by maximizing the posterior expected utility with no constraint.

On average, a smaller sample size and lower signal-to-noise ratio lead to a greater ACRisk. Interestingly, an appropriate level of the safety constraint (around 0.05 in this simulation) achieves a greater average value compared to maximizing the posterior expected value with no constraint. This is especially true when the sample size is small and/or the signal-to-noise ratio is low. In such settings, the safety constraint regularizes the policy optimization, only modifying the existing policy for those who are expected to benefit from a new policy with a high degree of certainty.

Prior in extrapolation. Next, we investigate the influence of prior parameters in GPs on the performance of the proposed methodology under Scenario II where there is no covariate overlap. Specifically, we consider the scale parameter l and the variance parameter σ_0^2 , which determine the smoothness of

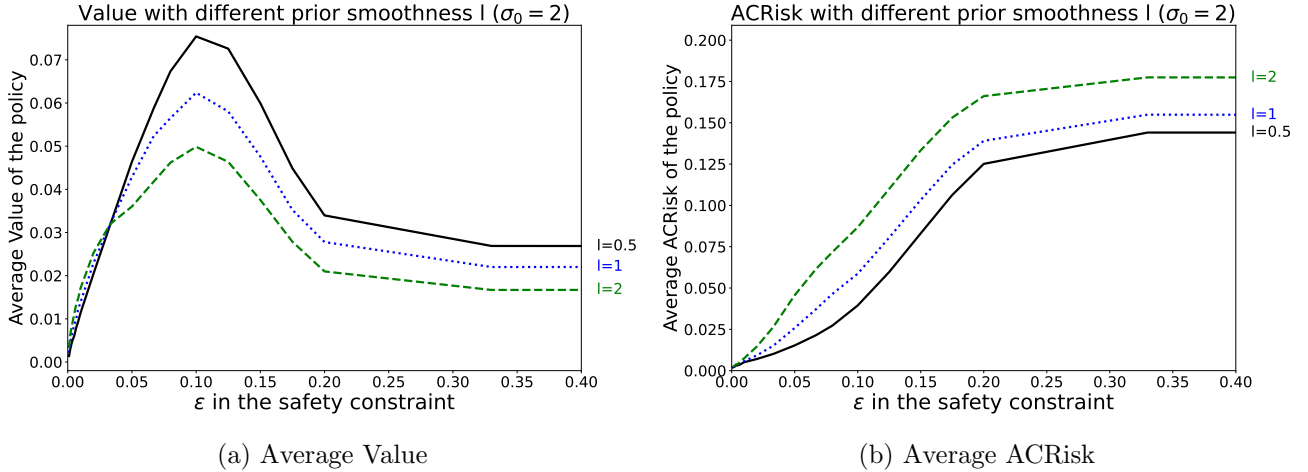


Figure 3: Average Value (left panel) and ACRisk (right panel) for learned policies using data without covariate overlap, varying the safety constraint ϵ and prior smoothness for the CATE l (a greater value corresponds to a greater degree of prior smoothness).

CATE and prior strength, respectively. Recall that a greater value of l implies a smoother function, while a smaller value of σ_0^2 corresponds to a stronger prior belief. We fix the sample size to 200 and use a low signal-to-noise ratio when generating the data.

Figure 3a shows the average value of the learned policy under different prior smoothness. In general, the value of learned policy tends to decrease as the prior smoothness increases. However, when the safety constraint is strong (i.e., ϵ is small), the value of the learned policy with stronger prior smoothness is slightly greater. A small value of ϵ implies that we only wish to change the baseline policy for a set of covariates that correspond to large CATEs. A smoother prior leads to a more conservative estimate of the CATE and can better identify such covariates.

Furthermore, Figure 3b shows that as the prior for the CATE becomes smoother, we extrapolate further, leading to an increase in the average ACRisk. In Figure ?? of the appendix, we observe a similar pattern when varying the prior strength for estimating the CATE.

To summarize, our simulation study shows that the safety constraint on the PACRisk can effectively control the true ACRisk in policy learning, reducing the risk of harming specified subgroups. In addition, a moderately binding safety constraint can induce beneficial regularization and improve the average value of the learned policy, especially when the sample size is small and the signal-to-noise ratio is low.

6 Empirical Analysis of the HES Security Assessment

With our methodological development in hand, we now return to the analysis of the military security assessment described in Section 2. We will focus on learning a new rule to aggregate the 20 sub-model scores into one overall security score, while keeping the original structure of the HES and only modifying the two-way and three-way tables used for the aggregation.

6.1 Setup

To formalize our problem, let $X^{(k)} \in [1, 5]$ denote the k -th sub-model scores with $k \in \{1, 2, \dots, 20\}$, where $\mathbf{X} \in \mathcal{X}$ denotes the whole 20-dimensional input vector. We use $S^{(i,j)} \in \{1, 2, 3, 4, 5\}$ to represent the i th score at the j th level where $i \in \{1, 2, \dots, n_j\}$ and $j \in \{1, 2, 3\}$ with n_j representing the total number of scores aggregated at the j -th level. We note that $X^{(k)} \neq S^{(1,k)}$ because the raw input score $X^{(k)}$ is rounded to obtain the first level score $S^{(1,k)}$. To apply the Bayesian safe policy learning method, we use the empirical CDF of \mathbf{X} as an approximate of its population CDF.

The output security score is denoted by $D \in \mathcal{D} = \{1, 2, 3, 4, 5\}$. We use $Y \in \{0, 1\}$ to represent one of three binary regional development outcomes measured in January, 1970: *regional safety*, *regional economy*, and *regional civic society*. These variables are calculated in Dell and Querubin (2018) with a latent class analysis on data from the HES, armed forces administrative records, and public opinion surveys. We analyze each outcome separately.

We consider a policy δ , which is a deterministic function that maps the inputs $\mathbf{x} \in \mathcal{X}$ (the 20 sub-model scores) to an output score $d \in \mathcal{D}$. We define two-way and three-way decision tables as the following functions that map integer-valued input scores to an integer-valued output score. Recall that each input/output score takes an integer value, ranging from 1 to 5.

$$\begin{aligned} T_2(\cdot, \cdot) &: \{1, 2, 3, 4, 5\}^2 \rightarrow \{1, 2, 3, 4, 5\}, \\ T_3(\cdot, \cdot, \cdot) &: \{1, 2, 3, 4, 5\}^3 \rightarrow \{1, 2, 3, 4, 5\}. \end{aligned} \tag{9}$$

Let \tilde{T}_2 and \tilde{T}_3 represent the baseline decision tables used in the existing HES. These existing rules are *monotonic*, meaning that a decision table with a greater input score never yields a smaller output score, holding the other input scores constant. Formally, a two-way decision table T_2 is monotonic if and only if we have $T_2(i_1, j_1) \leq T_2(i_2, j_2)$ for all $i_1, j_1, i_2, j_2 \in \{1, 2, 3, 4, 5\}$ and $i_1 \leq i_2, j_1 \leq j_2$. Similarly, a three-way decision table T_3 is monotonic if and only if we have $T_3(i_1, j_1, k_1) \leq T_3(i_2, j_2, k_2)$ for all $i_1, j_1, k_1, i_2, j_2, k_2 \in \{1, 2, 3, 4, 5\}$ and $i_1 \leq i_2, j_1 \leq j_2, k_1 \leq k_2$. Recall that the sub-model scores are ordered so that lower values are “worse.” Thus, the monotonicity condition is reasonable because higher sub-model scores should not make a region less secure. We will require that our learned decision tables also satisfy this monotonicity condition.

6.2 Learning to aggregate military, economic, and political sub-models

We begin by learning a single decision table while keeping the other tables of the HES. In particular, we consider learning a new third-level three-way decision table T_3 that aggregates three scores — the Military, Political, and Social Economic models — and produces the final output security score D (see Figure 1).

We use separate GPs with a logit link function g to model the expected outcome under different decisions (see Section 4.3). Specifically, we assume the model given in Equation (7) where $d = 1, 2, 3, 4, 5$.

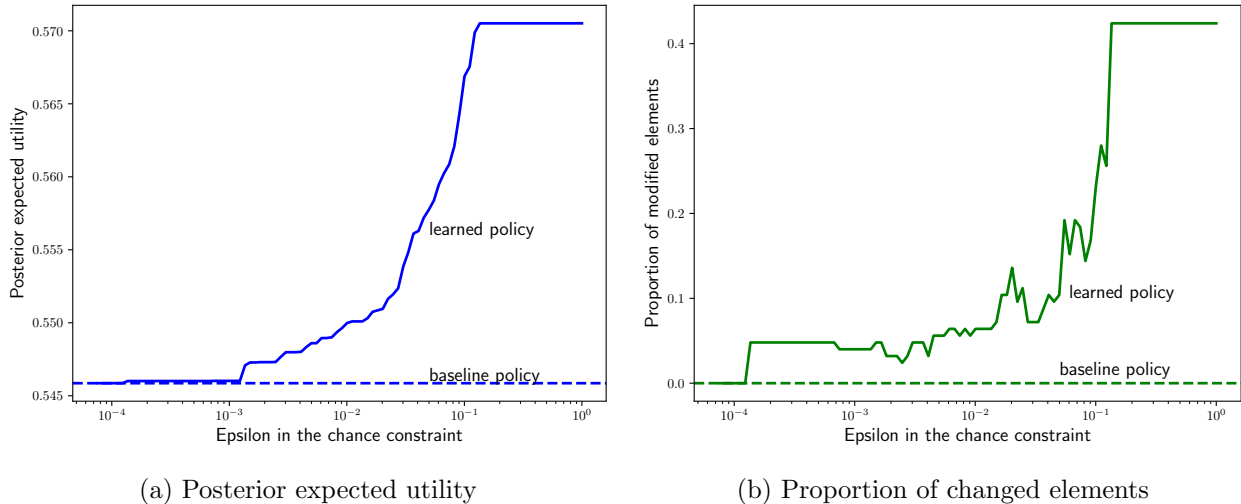


Figure 4: The posterior expected utility of the learned policy (left panel) and the proportion of elements in the three-way table changed by the learned policy (right panel) under different values of ϵ , when regional *safety* development is the outcome. A weaker safety constraint (i.e., a greater value of ϵ) leads to a greater difference between the baseline and learned policies. The posterior expected utility also becomes greater.

We use f_0 to model the expected outcome under the decision $D = 1$, whereas f_k with $k = 1, 2, 3, 4$ is used to model the effect between two adjacent decisions.

We set the prior mean function for all the GPs to zero, i.e., $m(x) = 0$, implying that all potential outcomes are distributed as Bernoulli with probability $1/2$. For the kernel function of the GP, we use a Matern kernel with $\nu = 3/2, l = 1, \sigma_0^2 = 4$ (see Equation (??)). This corresponds to a weak prior, implying that with more than 90% probability, $f_k(\cdot)$ is no less smooth than a Lipschitz function with the Lipschitz constant of 10.95. Appendix ?? presents a sensitivity analysis where we use larger/smaller values of l to induce more/less extrapolation. Overall, these results are consistent with our main findings that are presented below.

Optimizing a single decision table in our application is not computationally demanding. Therefore, we use the Gurobi solver to optimize Equation (5) over three-way monotonic decision tables. We use the military impacts on regional *safety*, *economy*, and *civic society* as separate binary outcomes and set the utility function to $u(D, Y) = Y$. Our utility only considers the outcome and does not penalize the use of a lower or higher security score.

Figure 4 shows how the results of our Bayesian safe policy learning procedure change with the safety constraint ϵ when the outcome is regional *safety*. Figure 4a shows the posterior expected utility of the learned policy, while Figure 4b presents the proportion of changed elements in the three-way table. We find that a weaker safety constraint (i.e., a greater value of ϵ) leads to a greater difference between the learned and baseline policies in terms of the changed elements of the three-way table. The learned policy also has a higher posterior expected utility when the safety constraint is weaker.

Figure 5 presents the relative difference in the partial dependence (PD) of the baseline and learned

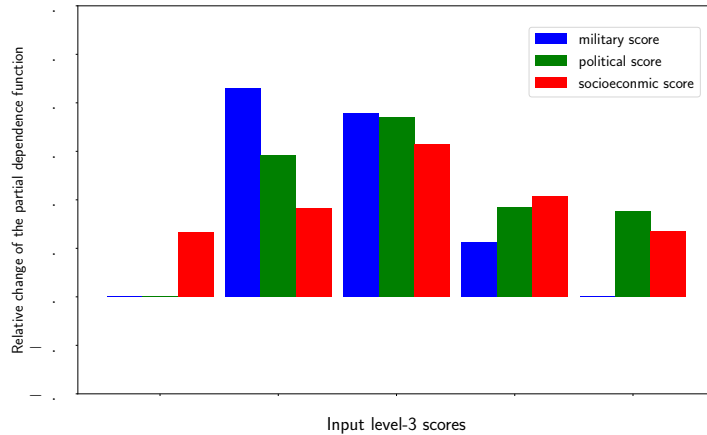


Figure 5: The relative change of the PD function from the baseline policy to the learned policy for $\epsilon = 0.1$. Each block corresponds to a different input of the PD function, and different colors corresponds to different level-3 scores. For example, the first blue bar in the first block corresponds to $\{I_{military}(1; T_3) - I_{military}(1; \tilde{T}_3)\} / I_{military}(1; \tilde{T}_3)$, where T_3 and \tilde{T}_3 are the learned and baseline policies, respectively.

policies with respect to the three level-3 scores. The PD function measures the dependence of the output security score on the level-3 scores, i.e., $S^{(3,1)}, S^{(3,2)}, S^{(3,3)}$, by computing the marginal expected output of the policy given certain input scores (Friedman, 2001; Greenwell et al., 2018). For example, the PD function for policy $\delta(\cdot; T_3)$ with respect to level-3 military score $S^{(3,1)}$ is computed as,

$$I_{military}(x; T_3) = \frac{1}{n} \sum_{i=1}^n T_3(x, S_i^{(3,2)}, S_i^{(3,3)}).$$

We find the percent change in the PD function between the learned and baseline policies are mostly positive. That is, the expected output security score under the learned policy is generally higher than the baseline policy for all three level-3 input scores. Recall that a higher security score signifies that a region should not be targeted, so increasing the scores would be likely to decrease the frequency of airstrikes, and potentially improve the regional outcome. This finding is consistent with that of Dell and Querubin (2018): airstrikes increased the military and political activities of the communist insurgency, decreasing regional safety and the regional economy.

We further compute the PD importance (Greenwell et al., 2018) of the military, political, and socioeconomic level-3 scores under the learned policy as a function of the safety constraint ϵ , using the three different outcomes. The PD importance measures the degree to which a PD function is sensitive to the input. A small PD importance means that the output score does not strongly depend on the input. For ease of interpretation, we scale the PD importance of level-3 scores for each policy so that they sum to one, allowing us to compare the PD importance of level-3 scores across different policies.

Figure 6 compares the scaled PD importance of each factor (denoted by different colors) between the baseline (dotted lines) and learned (solid lines) policies as a function of the strength of the safety constraint ϵ . The figure shows a consistent pattern, in which the new learned policies upweight the

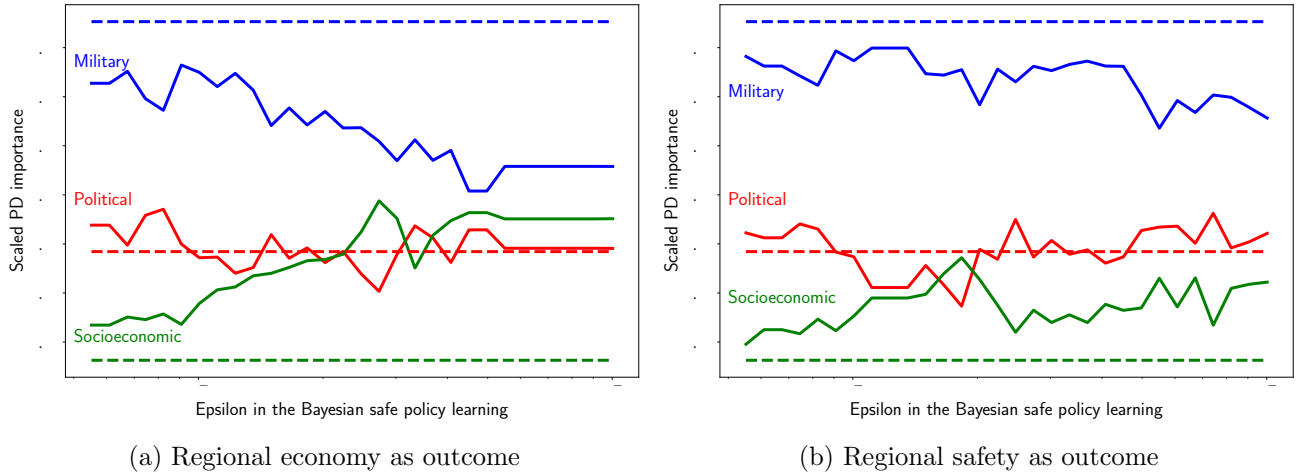


Figure 6: The scaled Partial Dependence (PD) importance of level-3 scores of the learned policy, as a function of the ϵ . The solid line corresponds to the learned policy, and the dashed line indicates the baseline policy. Lines with different colors shows the PD importance of different level-3 scores.

socioeconomic model and downweight the military model, when both the regional economy and regional safety are used as outcomes. Figure ?? in the appendix further investigates the PD importance of different factors in learned policy with civic society outcomes. Overall, our analysis suggests that the HES over-emphasized the importance of the military model for all three types of outcomes.

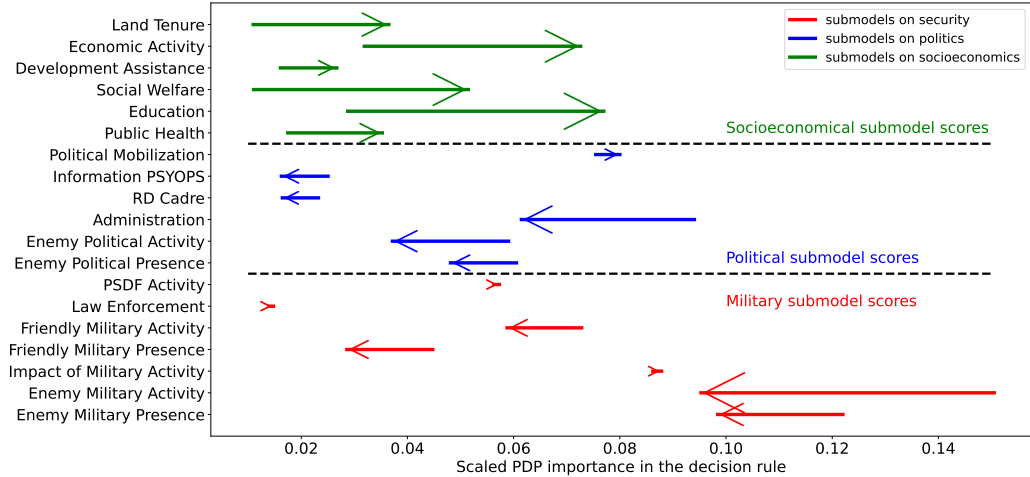
6.3 Learning the entire scoring system

Next, we consider learning both the two-way and three-way tables through all three levels of aggregation. In other words, we consider a policy class with the same aggregation structure as in the original HES, but allows the two-way and three-way tables to be modified. Formally, we consider the following policy class, $\Delta_3 = \{\delta(\cdot; T_2, T_3) : T_2, T_3 \text{ is monotonic}\}$. We use the same posterior CATE draws obtained in the previous analysis.

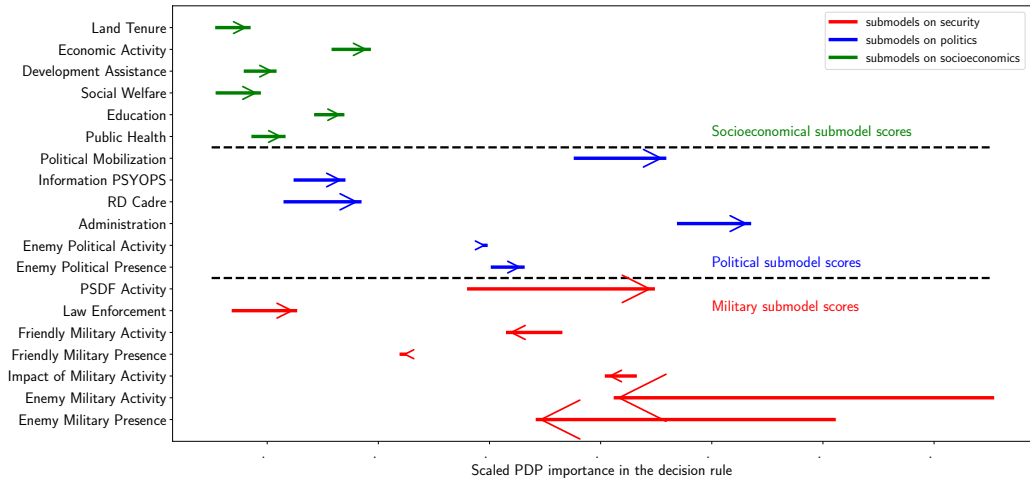
Unlike Section 6.2, this complex policy class makes it difficult to directly optimize the objective. In Appendix ??, we develop an optimization method based on directed acyclic graph (DAG) partitioning to solve this specific problem. As in the previous analysis, we compute the PD importance measure for each sub-model score.

As the policy class Δ_3 is large and contains many different policies, it is difficult to directly interpret the obtained policy through the learned decision tables. Therefore, we use the PD importance measure to understand how the data-derived policy differs from the HES. Figure 7 presents the relative importance of the sub-model scores under the baseline and optimal policies with a safety constraint $\epsilon = 0.1$. Each plot shows the scaled PD importance of the 19 different sub-model scores under the baseline and learned policies for the three different outcomes: regional safety, economy, and civic society. Each arrow shows how the scaled PD importance changes from the baseline policy to the learned policy.

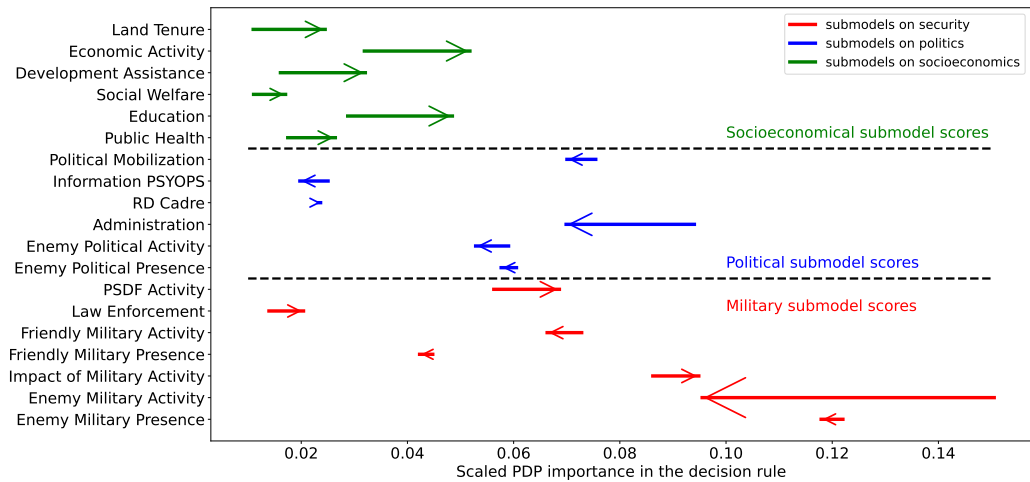
We find that when the outcome is either regional economy or civic society (Figures 7a and 7b), the learned policy puts less weight on the security sub-model scores than the baseline policy, with



(a) Regional economy as outcome



(b) Regional civic society as outcome



(c) Regional safety as outcome

Figure 7: The scaled PD importance of 19 different sub-model scores in the learned policy ($\epsilon = 0.1$) and baseline policy with different outcomes. Each arrow indicates the change of the scaled PDP importance from the baseline policy to the learned policy.

particularly large declines in the relative importance of enemy military activity and presence. Note, however, that this is partially offset by an increase in the relative importance of PSDF (People’s Self-Defense Force) activity and law enforcement.

In contrast, the socioeconomic sub-model scores are more important when targeting all three outcomes, and particularly so when targeting the economic outcome. Finally, the change in the relative importance of the political sub-model scores is more mixed; their importance only changes slightly when targeting regional safety (Figure 7c). It generally declines when targeting the regional economy, and increases when targeting regional civic society.

7 Concluding Remarks

In this paper, we propose a new notion of the average conditional risk (ACRisk), which represents the population proportion of groups that would be worse off under a new policy than under the baseline policy. We then develop a Bayesian safe policy learning methodology that limits this risk. We separate the estimation of heterogeneous treatment effects from the optimization of policies, enabling the use of flexible Bayesian nonparametric models while considering a complex policy class.

We apply the proposed methodology to the HES, a military security assessment used during the Vietnam War to guide airstrike decisions for USAF commanders. Substantively, our analysis shows that the HES—which saw active use during the war—attached too much importance to the military security scores. In contrast, the Bayesian safe policy assigns greater weights to socioeconomic factors. We also develop a stochastic optimization algorithm that is generally applicable to monotonic decision tables. Given the popularity of such decision rules in public policy and other settings, we believe that our optimization algorithm is of independent interest.

There are several directions for further research. First, while we take a Bayesian approach, one may consider a frequentist approach to controlling the ACRisk in policy learning. Second, our simulation study suggests that the posterior ACRisk constraint plays a role of regularization in policy optimization and an appropriate level of risk constraint can improve the average value of the learned policy. Better understanding how regularization improves policy learning is an important next step. Third, it is of interest to extend the proposed Bayesian policy learning framework to other types of constraints such as fairness and budget constraints.

References

- Athey, S. and Wager, S. (2021). Policy learning with observational data. *Econometrica*, 89(1):133–161.
- Bai, C., Wang, L., Yang, Z., Deng, Z., Garg, A., Liu, P., and Wang, Z. (2022). Pessimistic bootstrapping for uncertainty-driven offline reinforcement learning. *arXiv preprint arXiv:2202.11566*.
- Ben-Michael, E., Greiner, D. J., Imai, K., and Jiang, Z. (2021). Safe policy learning through extrapolation: Application to pre-trial risk assessment. *arXiv preprint arXiv:2109.11679*.

- Ben-Michael, E., Imai, K., and Jiang, Z. (2024). Policy learning with counterfactual asymmetric utilities. *Journal of the American Statistical Association*.
- Beygelzimer, A. and Langford, J. (2009). The offset tree for learning with partial labels. In *Proceedings of the 15th ACM SIGKDD international conference on Knowledge discovery and data mining*, pages 129–138.
- Branson, Z., Rischard, M., Bornn, L., and Miratrix, L. W. (2019). A nonparametric bayesian methodology for regression discontinuity designs. *Journal of Statistical Planning and Inference*, 202:14–30.
- Buckman, J., Gelada, C., and Bellemare, M. G. (2020). The importance of pessimism in fixed-dataset policy optimization. *arXiv preprint arXiv:2009.06799*.
- Carpenter, B., Gelman, A., Hoffman, M. D., Lee, D., Goodrich, B., Betancourt, M., Brubaker, M., Guo, J., Li, P., and Riddell, A. (2017). Stan: A probabilistic programming language. *Journal of statistical software*, 76(1).
- Chen, J. and Jiang, N. (2022). Offline reinforcement learning under value and density-ratio realizability: the power of gaps. *arXiv preprint arXiv:2203.13935*.
- Chipman, H. A., George, E. I., and McCulloch, R. E. (2010). Bart: Bayesian additive regression trees.
- Daddis, G. A. (2012). The problem of metrics: Assessing progress and effectiveness in the Vietnam War. *War in History*, 19(1):73–98.
- Delage, E. and Mannor, S. (2007). Percentile optimization in uncertain markov decision processes with application to efficient exploration. In *Proceedings of the 24th international conference on Machine learning*, pages 225–232.
- Delage, E. and Mannor, S. (2010). Percentile optimization for markov decision processes with parameter uncertainty. *Operations research*, 58(1):203–213.
- Dell, M. and Querubin, P. (2018). Nation building through foreign intervention: Evidence from discontinuities in military strategies. *The Quarterly Journal of Economics*, 133(2):701–764.
- Ding, P. and Li, F. (2018). Causal inference: a missing data perspective. *Statistical Science*, 33(2):214–237.
- Dudík, M., Langford, J., and Li, L. (2011). Doubly robust policy evaluation and learning. *Proceedings of the 28th International Conference on Machine Learning*.
- Farina, M., Giulioni, L., and Scattolini, R. (2016). Stochastic linear model predictive control with chance constraints – a review. *Journal of Process Control*, 44:53–67.

- Filar, J. A., Krass, D., and Ross, K. W. (1995). Percentile performance criteria for limiting average markov decision processes. *IEEE Transactions on Automatic Control*, 40(1):2–10.
- Friedman, J. H. (2001). Greedy function approximation: a gradient boosting machine. *Annals of statistics*, pages 1189–1232.
- Garcia, J. and Fernández, F. (2015). A comprehensive survey on safe reinforcement learning. *Journal of Machine Learning Research*, 16(1):1437–1480.
- Geibel, P. and Wyzotzki, F. (2005). Risk-sensitive reinforcement learning applied to control under constraints. *Journal of Artificial Intelligence Research*, 24:81–108.
- Greenwell, B. M., Boehmke, B. C., and McCarthy, A. J. (2018). A simple and effective model-based variable importance measure. *arXiv preprint arXiv:1805.04755*.
- Greiner, J., Halen, R., Stubenberg, M., and Griffin, C. L. (2020). Randomized control trial evaluation of the implementation of the psa-dmf system in dane county, wi.
- Hahn, P. R., Murray, J. S., and Carvalho, C. M. (2020). Bayesian regression tree models for causal inference: Regularization, confounding, and heterogeneous effects (with discussion). *Bayesian Analysis*, 15(3):965–1056.
- Hill, J. L. (2011). Bayesian nonparametric modeling for causal inference. *Journal of Computational and Graphical Statistics*, 20(1):217–240.
- Imai, K., Jiang, Z., Greiner, D. J., Halen, R., and Shin, S. (2023). Experimental evaluation of computer-assisted human decision-making: Application to pretrial risk assessment instrument (with discussion). *Journal of the Royal Statistical Society, Series A (Statistics in Society)*, 186(2):167–189.
- Jin, Y., Ren, Z., Yang, Z., and Wang, Z. (2022). Policy learning” without”overlap: Pessimism and generalized empirical bernstein’s inequality. *arXiv preprint arXiv:2212.09900*.
- Jin, Y., Yang, Z., and Wang, Z. (2021). Is pessimism provably efficient for offline rl? In *International Conference on Machine Learning*, pages 5084–5096. PMLR.
- Kallus, N. (2018). Balanced policy evaluation and learning. *Advances in neural information processing systems*, 31.
- Kallus, N. (2022). What’s the harm? sharp bounds on the fraction negatively affected by treatment. *arXiv preprint arXiv:2205.10327*.
- Kallus, N. and Zhou, A. (2021). Minimax-optimal policy learning under unobserved confounding. *Management Science*, 67(5):2870–2890.

- Kamath, P. S., Wiesner, R. H., Malinchoc, M., Kremers, W., Therneau, T. M., Kosberg, C. L., D’Amico, G., Dickson, E. R., and Kim, W. R. (2001). A model to predict survival in patients with end-stage liver disease. *Hepatology*, 33(2):464–470.
- Kasy, M. (2018). Optimal taxation and insurance using machine learning—sufficient statistics and beyond. *Journal of Public Economics*, 167:205–219.
- Kitagawa, T. and Tetenov, A. (2018). Who should be treated? empirical welfare maximization methods for treatment choice. *Econometrica*, 86(2):591–616.
- Lauer, J. (2017). *Creditworthy: A History of Consumer Surveillance and Financial Identity in America*. Columbia University Press.
- Li, A., Jiang, S., Sun, Y., and Pearl, J. (2022a). Unit selection: Learning benefit function from finite population data. *arXiv preprint arXiv:2210.08203*.
- Li, F., Ding, P., and Mealli, F. (2022b). Bayesian causal inference: A critical review. *arXiv preprint arXiv:2206.15460*.
- Li, L., Chu, W., Langford, J., and Schapire, R. E. (2010). A contextual-bandit approach to personalized news article recommendation. In *Proceedings of the 19th international conference on World wide web*, pages 661–670.
- Luedtke, A. R. and Van Der Laan, M. J. (2016). Statistical inference for the mean outcome under a possibly non-unique optimal treatment strategy. *Annals of statistics*, 44(2):713.
- Manski, C. F. (2007). Minimax-regret treatment choice with missing outcome data. *Journal of Econometrics*, 139(1):105–115.
- Mowbray, M., Petsagkourakis, P., del Rio-Chanona, E. A., and Zhang, D. (2022). Safe chance constrained reinforcement learning for batch process control. *Computers & chemical engineering*, 157:107630.
- Nahum-Shani, I., Smith, S. N., Spring, B. J., Collins, L. M., Witkiewitz, K., Tewari, A., and Murphy, S. A. (2018). Just-in-time adaptive interventions (jitais) in mobile health: key components and design principles for ongoing health behavior support. *Annals of Behavioral Medicine*, 52(6):446–462.
- Neyman, J. (1990 [1923]). On the application of probability theory to agricultural experiments. essay on principles. section 9. *Statistical Science*, 5(4):465–472.
- PACAF, H. Q. (1969). Tacc fragging procedures. *Project CHECO Southeast Asia Report*.
- Pu, H. and Zhang, B. (2020). Estimating optimal treatment rules with an instrumental variable: A partial identification learning approach. *arXiv preprint arXiv:2002.02579*.

- Qian, M. and Murphy, S. A. (2011). Performance guarantees for individualized treatment rules. *Annals of statistics*, 39(2):1180.
- Rashidinejad, P., Zhu, B., Ma, C., Jiao, J., and Russell, S. (2021). Bridging offline reinforcement learning and imitation learning: A tale of pessimism. *Advances in Neural Information Processing Systems*, 34:11702–11716.
- Rasmussen, C. E. and Williams, C. K. I. (2006). Gaussian processes for machine learning. The MIT Press.
- Rosenbaum, P. R. and Rubin, D. B. (1983). The central role of the propensity score in observational studies for causal effects. *Biometrika*, 70(1):41–55.
- Rubin, D. B. (1974). Estimating causal effects of treatments in randomized and nonrandomized studies. *Journal of educational Psychology*, 66(5):688.
- Rubin, D. B. (1980). Randomization analysis of experimental data: The fisher randomization test comment. *Journal of the American statistical association*, 75(371):591–593.
- Sato, M., Kimura, H., and Kobayashi, S. (2001). Td algorithm for the variance of return and mean-variance reinforcement learning. *Transactions of the Japanese Society for Artificial Intelligence*, 16(3):353–362.
- Schwarm, A. T. and Nikolaou, M. (1999). Chance-constrained model predictive control. *AIChE Journal*, 45(8):1743–1752.
- Schwartz, E. M., Bradlow, E. T., and Fader, P. S. (2017). Customer acquisition via display advertising using multi-armed bandit experiments. *Marketing Science*, 36(4):500–522.
- Shi, L., Li, G., Wei, Y., Chen, Y., and Chi, Y. (2022). Pessimistic q-learning for offline reinforcement learning: Towards optimal sample complexity. *arXiv preprint arXiv:2202.13890*.
- Swaminathan, A. and Joachims, T. (2015). Batch learning from logged bandit feedback through counterfactual risk minimization. *The Journal of Machine Learning Research*, 16(1):1731–1755.
- Taddy, M., Gardner, M., Chen, L., and Draper, D. (2016). A nonparametric bayesian analysis of heterogenous treatment effects in digital experimentation. *Journal of Business & Economic Statistics*, 34(4):661–672.
- Tang, L., Rosales, R., Singh, A., and Agarwal, D. (2013). Automatic ad format selection via contextual bandits. In *Proceedings of the 22nd ACM international conference on Information & Knowledge Management*, pages 1587–1594.

- Uehara, M. and Sun, W. (2021). Pessimistic model-based offline reinforcement learning under partial coverage. *arXiv preprint arXiv:2107.06226*.
- Vakili, S. and Zhao, Q. (2015). Mean-variance and value at risk in multi-armed bandit problems. In *2015 53rd Annual Allerton Conference on Communication, Control, and Computing (Allerton)*, pages 1330–1335. IEEE.
- Vitus, M. P., Zhou, Z., and Tomlin, C. J. (2015). Stochastic control with uncertain parameters via chance constrained control. *IEEE Transactions on Automatic Control*, 61(10):2892–2905.
- Wei, D., Nair, R., Dhurandhar, A., Varshney, K. R., Daly, E. M., and Singh, M. (2022). On the safety of interpretable machine learning: A maximum deviation approach. *arXiv preprint arXiv:2211.01498*.
- Xie, T., Cheng, C.-A., Jiang, N., Mineiro, P., and Agarwal, A. (2021). Bellman-consistent pessimism for offline reinforcement learning. *Advances in neural information processing systems*, 34:6683–6694.
- Yan, Y., Li, G., Chen, Y., and Fan, J. (2022). The efficacy of pessimism in asynchronous q-learning. *arXiv preprint arXiv:2203.07368*.
- Yata, K. (2021). Optimal decision rules under partial identification. *arXiv preprint arXiv:2111.04926*.
- Yin, M. and Wang, Y.-X. (2021). Towards instance-optimal offline reinforcement learning with pessimism. *Advances in neural information processing systems*, 34:4065–4078.
- Zanette, A., Wainwright, M. J., and Brunskill, E. (2021). Provable benefits of actor-critic methods for offline reinforcement learning. *Advances in neural information processing systems*, 34:13626–13640.
- Zhang, B., Tsiatis, A. A., Davidian, M., Zhang, M., and Laber, E. (2012). Estimating optimal treatment regimes from a classification perspective. *Stat*, 1(1):103–114.
- Zhang, Y., Ben-Michael, E., and Imai, K. (2022). Safe policy learning under regression discontinuity designs. *arXiv preprint arXiv:2208.13323*.
- Zhao, Y., Zeng, D., Rush, A. J., and Kosorok, M. R. (2012). Estimating individualized treatment rules using outcome weighted learning. *Journal of the American Statistical Association*, 107(499):1106–1118.
- Zhou, X., Mayer-Hamblett, N., Khan, U., and Kosorok, M. R. (2017). Residual weighted learning for estimating individualized treatment rules. *Journal of the American Statistical Association*, 112(517):169–187.
- Zhou, Z., Athey, S., and Wager, S. (2022). Offline multi-action policy learning: Generalization and optimization. *Operations Research*.

Supplementary Appendix for “Bayesian Safe Policy Learning with Chance Constrained Optimization: Application to Military Security Assessment during the Vietnam War”

S1 Two-way and three-way decision tables used in the HES

Input 2	↑					
5		3	3	4	4	5
4		2	3	3	4	4
3		2	2	3	3	4
2		1	2	2	3	3
1		1	1	2	2	3
	↓	1	2	3	4	5
	→	Input 1				

Figure S1: The two-way table used in the Hamlet Evaluation System for aggregating two input scores. The (i, j) element in the table above shows the output score when the first input is i and the second input is j .

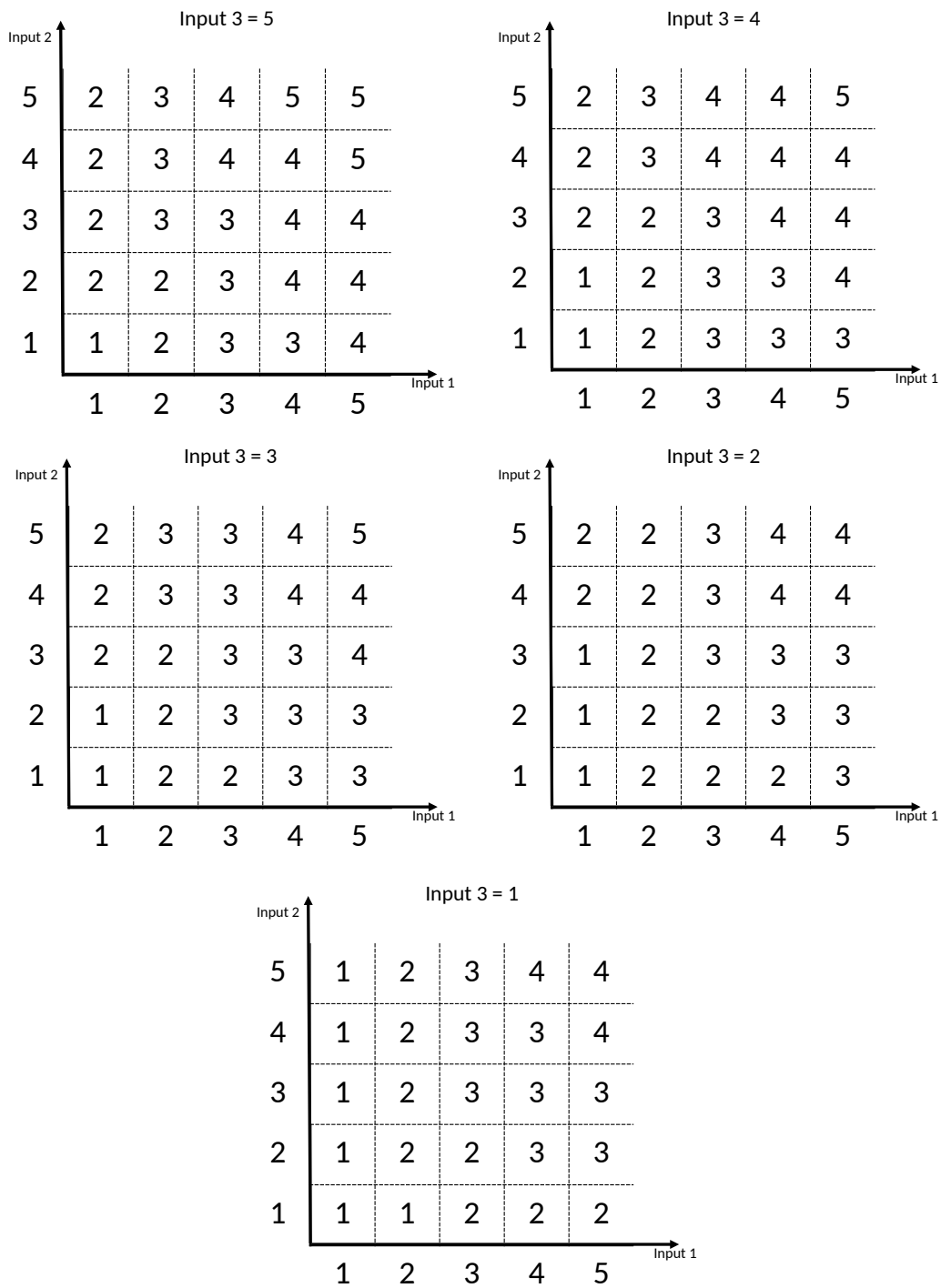


Figure S2: Three-way decision tables used in the HES. Each figure fixes the third input score and shows the output score for different combination of the first two inputs.

S2 Additional summaries of the HES

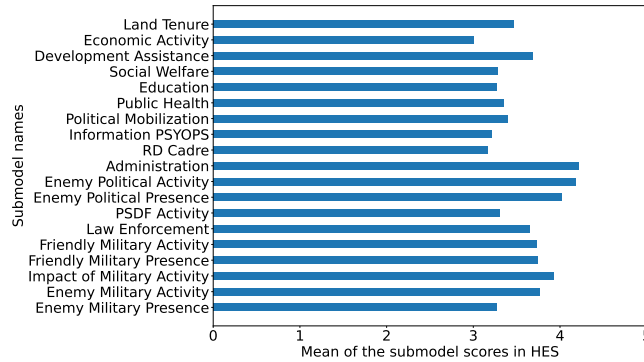


Figure S3: The mean of each sub-model score across the 1954 regions

Variable	Value
Number of regions	1954
Number of regions being attacked	1024
Average security score	3.34
Average regional safety outcome	0.53
Average regional economy outcome	0.51
Average civic society outcome	0.43

Table S1: Summary statistics on key measures

S3 Proof of Theorem ??

We wish to show that the original chance-constraint optimization problem (see Equation (??))

$$\delta_{\text{safe}} = \underset{\delta \in \Delta}{\operatorname{argmax}} \quad \mathbb{E}[V(\delta; \Theta) \mid \{Z_i\}_{i=1}^n], \quad (\text{S1})$$

$$\text{subject to} \quad \mathbb{E}\left[R(\delta, \tilde{\delta}; \Theta) \mid \{Z_i\}_{i=1}^n\right] \leq \epsilon, \quad (\text{S2})$$

can be equivalently written as,

$$\delta_{\text{safe}} = \underset{\delta \in \Delta}{\operatorname{argmax}} \quad \sum_{k=0}^{K-1} \int I(\delta(\mathbf{x}) = k) b_k(\mathbf{x}) dF(\mathbf{x}) \quad (\text{S3})$$

$$\text{subject to} \quad \sum_{k=0}^{K-1} \int I(\delta(\mathbf{x}) = k) r_k(\mathbf{x}) dF(\mathbf{x}) \leq \epsilon, \quad (\text{S4})$$

where $F(\mathbf{x})$ be the CDF of the covariate \mathbf{X} , and

$$\begin{aligned}\tau_k(\mathbf{x}, \boldsymbol{\theta}) &:= \mathbb{E} \left[u(k, Y(k)) - u(\tilde{\delta}(\mathbf{x}), Y(\tilde{\delta}(\mathbf{x}))) \mid \mathbf{X} = \mathbf{x}, \boldsymbol{\theta} = \boldsymbol{\theta} \right], \\ b_k(\mathbf{x}) &:= \mathbb{E} [\tau_k(\mathbf{x}, \boldsymbol{\theta}) \mid \{Z_i\}_{i=1}^n], \\ r_k(\mathbf{x}) &:= \mathbb{P} (\tau_k(\mathbf{x}, \boldsymbol{\theta}) < 0 \mid \{Z_i\}_{i=1}^n).\end{aligned}$$

We first show that the constraint given in Equation (S2) is equivalent to Equation (S4). By the definition of the posterior average conditional risk, we have

$$\begin{aligned}R(\delta, \tilde{\delta}; \boldsymbol{\theta}) &= \mathbb{P} \left(\mathbb{E} [u(\delta(\mathbf{X}), Y(\delta(\mathbf{X}))) \mid \mathbf{X}, \boldsymbol{\theta}] < \mathbb{E} [u(\tilde{\delta}(\mathbf{X}), Y(\tilde{\delta}(\mathbf{X}))) \mid \mathbf{X}, \boldsymbol{\theta}] \mid \boldsymbol{\theta} \right) \\ &= \mathbb{P} \left(\mathbb{E} [u(\delta(\mathbf{X}), Y(\delta(\mathbf{X}))) - u(\tilde{\delta}(\mathbf{X}), Y(\tilde{\delta}(\mathbf{X}))) \mid \mathbf{X}, \boldsymbol{\theta}] < 0 \mid \boldsymbol{\theta} \right) \\ &= \mathbb{P} \left(\sum_{k=0}^{K-1} \tau_k(\mathbf{X}, \boldsymbol{\theta}) I(\delta(\mathbf{X}) = k) < 0 \mid \boldsymbol{\theta} \right)\end{aligned}\tag{S5}$$

Therefore, Equation (S2) can be written as follows. For clarity, we use subscripts to explicitly indicate the random variables with respect to which each expectation is taken.

$$\begin{aligned}& \mathbb{E}_{\boldsymbol{\theta}} \left[R(\delta, \tilde{\delta}; \boldsymbol{\theta}) \mid \{Z_i\}_{i=1}^n \right] \\ &= \mathbb{E}_{\boldsymbol{\theta}} \left[\mathbb{P}_{\mathbf{X}} \left(\sum_{k=0}^{K-1} \tau_k(\mathbf{X}, \boldsymbol{\theta}) I(\delta(\mathbf{X}) = k) < 0 \mid \boldsymbol{\theta} \right) \mid \{Z_i\}_{i=1}^n \right] \\ &= \mathbb{E}_{\boldsymbol{\theta}} \left[\mathbb{E}_{\mathbf{X}} \left[I \left\{ \sum_{k=0}^{K-1} \tau_k(\mathbf{X}, \boldsymbol{\theta}) I(\delta(\mathbf{X}) = k) < 0 \right\} \mid \boldsymbol{\theta} \right] \mid \{Z_i\}_{i=1}^n \right] \\ &= \mathbb{E}_{\mathbf{X}, \boldsymbol{\theta}} \left[I \left\{ \sum_{k=0}^{K-1} \tau_k(\mathbf{X}, \boldsymbol{\theta}) I(\delta(\mathbf{X}) = k) < 0 \right\} \mid \{Z_i\}_{i=1}^n \right] \\ &= \mathbb{E}_{\mathbf{X}} \left[\mathbb{E}_{\boldsymbol{\theta}} \left[I \left\{ \sum_{k=0}^{K-1} \tau_k(\mathbf{X}, \boldsymbol{\theta}) I(\delta(\mathbf{X}) = k) < 0 \right\} \mid \{Z_i\}_{i=1}^n, \mathbf{X} \right] \mid \{Z_i\}_{i=1}^n \right] \\ &= \mathbb{E}_{\mathbf{X}} \left[\sum_{k=0}^{K-1} I(\delta(\mathbf{X}) = k) \mathbb{E}_{\boldsymbol{\theta}} \left[I \{ \tau_k(\mathbf{X}, \boldsymbol{\theta}) < 0 \} \mid \{Z_i\}_{i=1}^n, \mathbf{X} \right] \mid \{Z_i\}_{i=1}^n \right] \\ &= \mathbb{E}_{\mathbf{X}} \left[\sum_{k=0}^{K-1} I(\delta(\mathbf{X}) = k) r_k(\mathbf{X}) \mid \{Z_i\}_{i=1}^n \right] \\ &= \sum_{k=0}^{K-1} \int I(\delta(\mathbf{x}) = k) r_k(\mathbf{x}) dF(\mathbf{x}),\end{aligned}$$

where the third and fourth equalities follow from the law of iterated expectation, and the fifth equality uses the fact that there is only one non-zero term in the summation term $\sum_{k=0}^{K-1} \tau_k(\mathbf{X}, \boldsymbol{\theta}) I(\delta(\mathbf{X}) = k)$, leading to the simplification of the indicator function.

Similarly, for the optimization target, we have

$$\begin{aligned}
& \mathbb{E}[V(\delta; \Theta) \mid \{Z_i\}_{i=1}^n] \\
&= \mathbb{E}[u(\delta(\mathbf{X}), Y(\delta(\mathbf{X}))) \mid \{Z_i\}_{i=1}^n] \\
&= \mathbb{E}_{\mathbf{X}} \left[\mathbb{E}_Y \{u(\delta(\mathbf{X}), Y(\delta(\mathbf{X}))) \mid \{Z_i\}_{i=1}^n, \mathbf{X}\} \mid \{Z_i\}_{i=1}^n \right] \\
&= \mathbb{E}_{\mathbf{X}} \left[\mathbb{E}_Y \left\{ \sum_{k=0}^{K-1} u(\delta(\mathbf{X}), Y(k)) I(\delta(\mathbf{X}) = k) \mid \{Z_i\}_{i=1}^n, \mathbf{X} \right\} \mid \{Z_i\}_{i=1}^n \right] \\
&= \mathbb{E}_{\mathbf{X}} \left[\mathbb{E}_{\Theta} \left\{ \sum_{k=0}^{K-1} \tau_k(\mathbf{X}, \Theta) I(\delta(\mathbf{X}) = k) \mid \{Z_i\}_{i=1}^n, \mathbf{X} \right\} \mid \{Z_i\}_{i=1}^n \right] + \text{const.} \\
&= \mathbb{E}_{\mathbf{X}} \left[\sum_{k=0}^{K-1} I(\delta(\mathbf{X}) = k) b_k(\mathbf{X}) \mid \{Z_i\}_{i=1}^n \right] + \text{const.} \\
&= \sum_{k=0}^{K-1} \int I(\delta(\mathbf{x}) = k) b_k(\mathbf{x}) dF(\mathbf{x}) + \text{const.}
\end{aligned} \tag{S6}$$

where const. represents the term that is not a function of δ . In Equation (S6), the expectation is taken over the distribution of \mathbf{X} , the posterior distribution of Θ , and the conditional distribution of Y given \mathbf{X}, Θ . This completes the proof. \square

S4 BART and GP for Bayesian Inference on the CATE

Below, we consider BART and GP for Bayesian inference on these parameters $\{f_k\}_{k=0}^{K-1}$. Specifically, we sample from the posterior distribution of $\{f_k\}_{k=0}^{K-1}$ and apply Algorithm ?? to find a safe policy.

Bayesian Additive Regression Trees (BART). BART is a popular Bayesian nonparametric model that is commonly used for causal inference, especially to estimate the CATE (Taddy et al., 2016; Hahn et al., 2020). In general, BART excels in learning complex nonlinear relations while it is often poor at extrapolating. Thus, BART may be a suitable choice when there exists a substantial covariate overlap between treatment conditions.

We use a BART to model each f_k for $k \in \{0, 1, \dots, K-1\}$ as the sum of L regression trees, i.e., $f_k(\mathbf{x}) = \sum_{\ell=1}^L g_{k\ell}(\mathbf{x}; T_{k\ell}, P_{k\ell})$ where $g_{k\ell}(\cdot)$ is the ℓ -th regression tree with parameter $T_{k\ell}$ and $P_{k\ell}$ denoting the structure of the regression tree and the parameters in the terminal nodes, respectively. Thus, the parameter Θ consists of $\{T_{k\ell}, P_{k\ell}\}_{1 \leq \ell \leq L, 0 \leq k \leq K-1}$ as well as σ^2 . We draw posterior samples for $\{T_{k\ell}, P_{k\ell}\}_{1 \leq \ell \leq L}$ using an MCMC algorithm once a prior distribution is specified (Chipman et al., 2010).

Gaussian Process Regression. Another popular Bayesian nonparametric model is Gaussian Process regression (GP). GP has a greater degree of smoothness than BART, making it more suitable for extrapolation (Rasmussen and Williams, 2006; Branson et al., 2019). Therefore, we should consider using GP when the overlap of covariates between treatment conditions is poor.

As in the case of BART, we use a GP to model each f_k . Specifically, f_k is assumed to be a random function based on a collection of Gaussian processes. To conduct Bayesian inference on f_k , we specify a prior for f_k by giving the mean function $\mu_k(\cdot)$ and kernel function $K_k(\cdot, \cdot)$ and obtain posterior samples of f_k using the MCMC algorithm (Rasmussen and Williams, 2006; Branson et al., 2019).

When strong prior information is unavailable, we can set $\mu_k(\cdot) = 0$ for $k \geq 1$ which corresponds to no treatment effect. For the kernel function, which determines the covariance between $f_k(\mathbf{x}_1), f_k(\mathbf{x}_2)$ for any $\mathbf{x}_0, \mathbf{x}_1 \in \mathcal{X}$, we can, for example, use Matern kernels:

$$K_{\text{Matern}}(\mathbf{x}_1, \mathbf{x}_2) = \sigma_0^2 \frac{2^{1-\nu}}{\Gamma(\nu)} \left(\frac{\sqrt{2\nu} \|\mathbf{x}_1 - \mathbf{x}_2\|}{\ell} \right)^\nu B_\nu \left(\frac{\sqrt{2\nu} \|\mathbf{x}_1 - \mathbf{x}_2\|}{\ell} \right) \quad (\text{S7})$$

where l is the scale parameter, σ_0^2 is the variance parameter, B_ν is the modified Bessel function of the second kind, and ν is the smoothness parameter. The hyperparameters in the Matern kernels can be selected based on prior knowledge about the smoothness of $f_k(\cdot)$. For example, to make f_k more smooth, we can increase the scale and smoothness parameters. In general, ℓ and ν determine the prior knowledge about the smoothness of f , while σ_0^2 determines the strength of this prior knowledge.

Extrapolation based on GP is similar to frequentist extrapolation methods that specify the model class by assuming a certain type of smoothness on the CATE under the robust optimization framework. For example, Ben-Michael et al. (2021) considers the case with two arms and assumes a Lipschitz constraint on the CATE, i.e., $|f_1(\mathbf{x}_1) - f_1(\mathbf{x}_2)| \leq c \|\mathbf{x}_1 - \mathbf{x}_2\|$. In our framework, if we specify the prior of $f_1(\mathbf{x})$ as a GP with mean function $m(\mathbf{x})$ that is c_1 Lipschitz, then the Matern kernel with scale parameter ℓ and smoothness parameter ν implies the following probabilistic Lipschitz condition:

$$\mathbb{P}(|f_1(\mathbf{x}_1) - f_1(\mathbf{x}_2)| > c_2 \|\mathbf{x}_1 - \mathbf{x}_2\|) \leq \sigma_0^2 \left\{ \left(1 + \frac{1}{\nu - 1} \right) \frac{1}{c_2^2 \ell^2} + \frac{c_1^2}{c_2^2} \right\}$$

Thus, there exists a direct relationship between the prior hyperparameter of GP and the smoothness of the underlying model.

S5 Additional simulation results

Here, we present additional detailed simulation results.

S5.1 Average value and ACRisk with different signal strength and prior strength

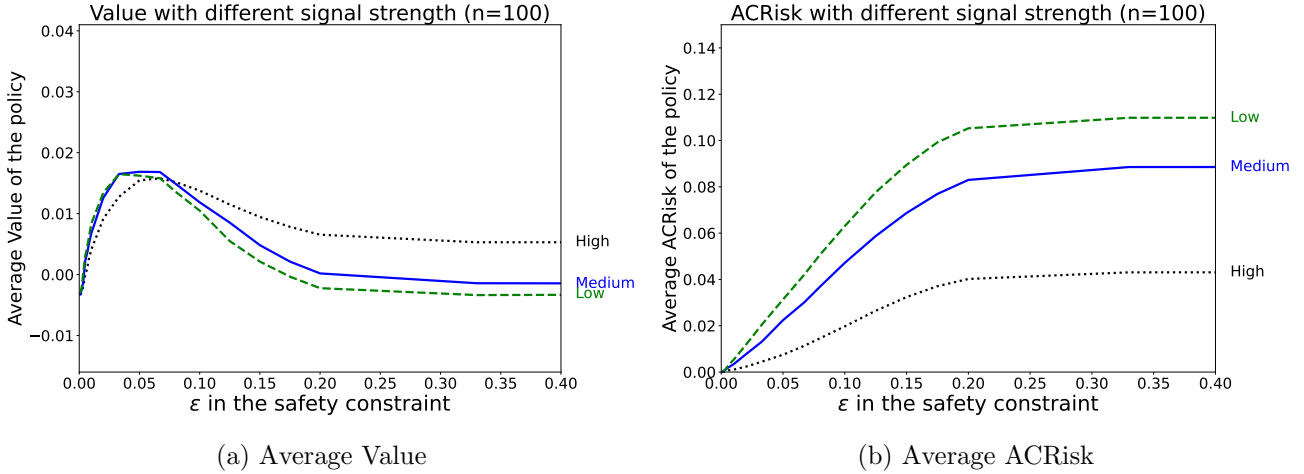


Figure S4: Average Value and ACRisk for learned policies using data with covariate overlap, varying the safety constraint and signal strength.

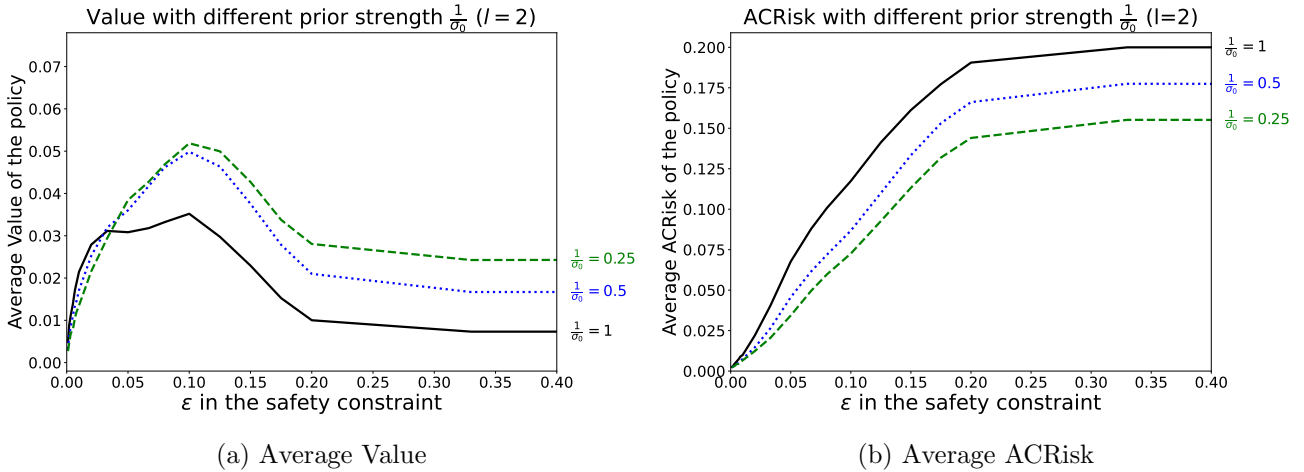


Figure S5: Average Value and ACRisk for learned policies using data without covariate overlap, varying the safety constraint and prior strength for the CATE.

S5.2 The tail distribution of the empirical ACRisk

In the main text, we discuss the average ACRisk of the learned policy in multiple simulations. However, we may also be interested in the tail distribution for the ACRisk of learned policy. Therefore, we inspect the 90 percentile of the ACRisk for the learned policy across 2000 simulations. Figures S6 and S7 show how the 90 percentile of the ACRisk changes with the sample size, signal strength, smoothness for prior of the CATE, and the strength of the prior.

Overall, we find the results similar to those presented in the main text. In figure S6, the 90 percentile of the ACRisk increases as the safety constraint ϵ increases before reaching a plateau that corresponds to the ACRisk obtained by maximizing the posterior expected utility with no constraint. A smaller sample size and lower signal-to-noise ratio lead to a greater ACRisk. For the setup without covariate overlap (figure S7), we see a smoother and stronger prior increase the ACRisk because the extrapolation is more aggressive.

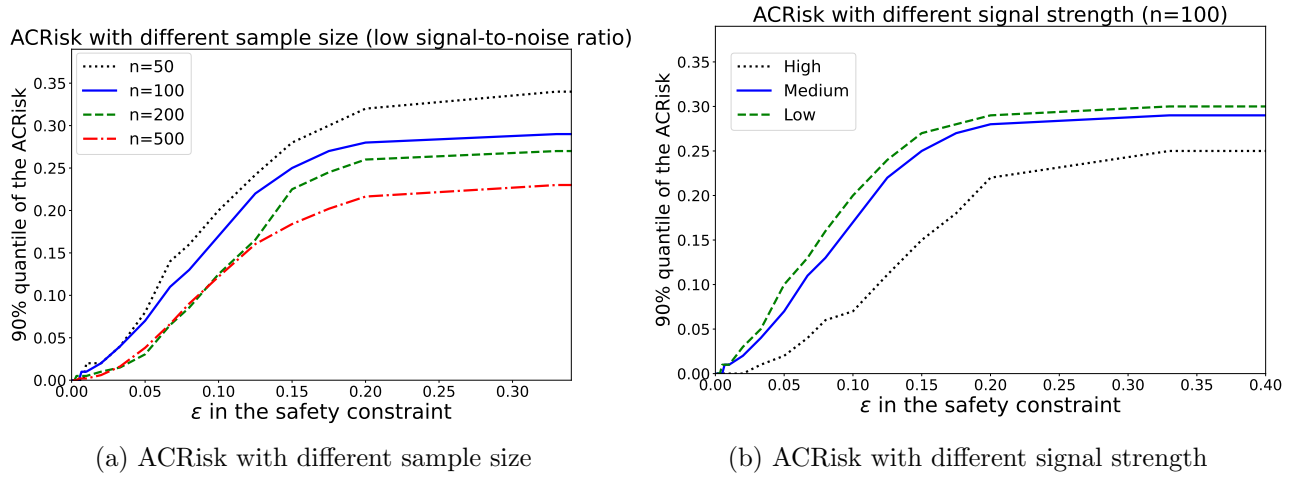


Figure S6: 90 % quantile of the ACRisk for learned policy among 2000 simulations. The CATE is estimated with BCF and covariates have overlap

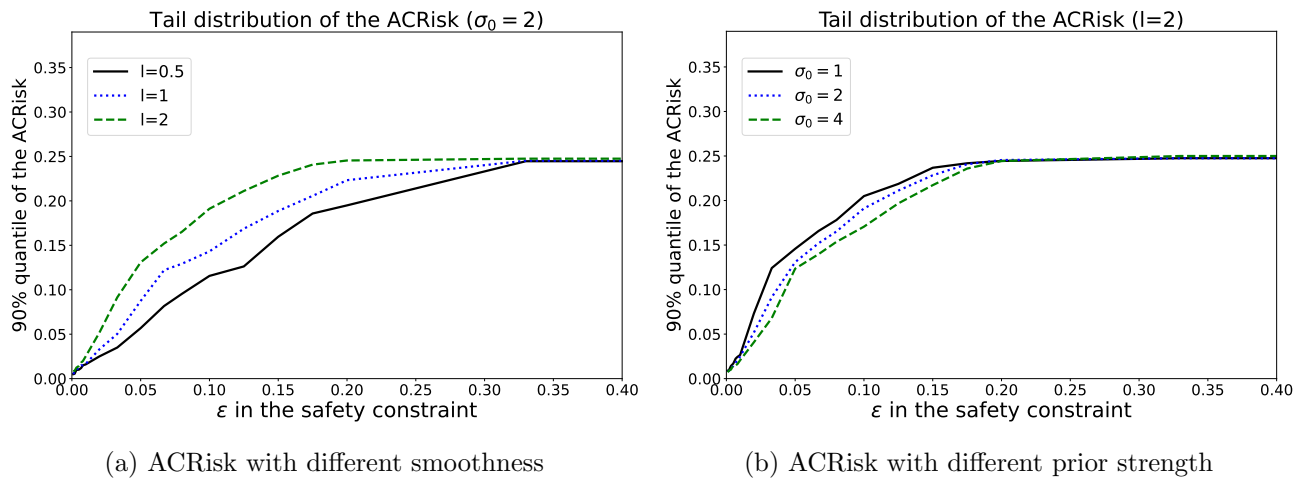
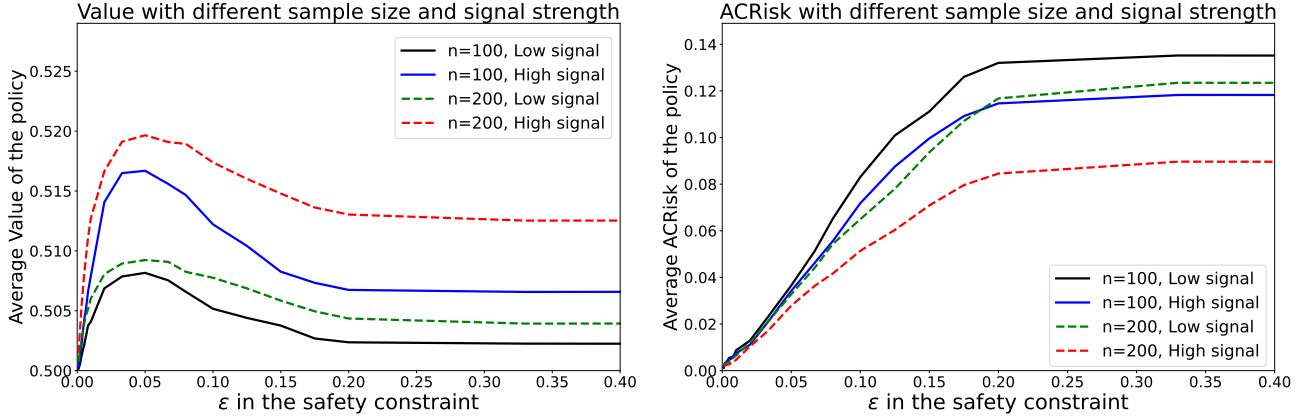


Figure S7: 90% quantile of the ACRisk for learned policy among 2000 simulations. The CATE is estimated with a GP and there is no covariate overlap.

S5.3 Simulation results with binary outcomes

The previous simulation design focused on continuous outcomes. Here, we present simulation results when the outcome is binary. We use a similar setup as in Section ?? where the covariates $\mathbf{X} = (X_1, X_2)$ and $X_1, X_2 \stackrel{i.i.d}{\sim} Uniform[-1, 1]$. We use the same Scenario I (with covariate overlap) and Scenario II



(a) Average Value with different sample size and signal strength (b) Average ACRisk with different sample size and signal strength

Figure S8: Average Value and ACRisk for the learned policy among 2000 simulations. The CATE is estimated with GP and covariates have overlap

(without covariate overlap) for generating the decision D in the data. For the outcome, we let

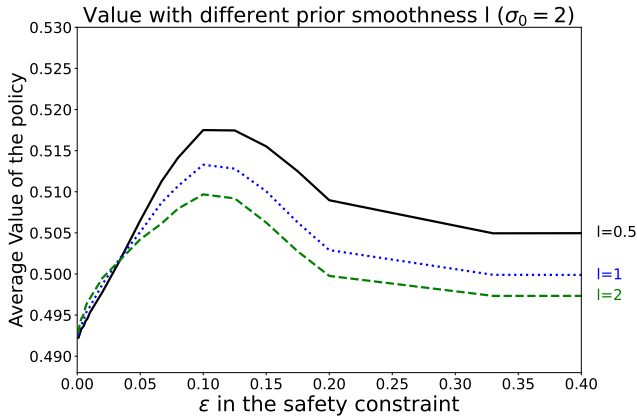
$$Y \mid \mathbf{X} \sim \text{Bernoulli} \left(\text{expit} \left(\frac{X_1}{2} + \frac{X_2}{2} + \gamma \{3I(X_1 > 0, X_2 > 0) - \frac{3}{2}\} D |X_1||X_2| \right) \right),$$

where we consider a strong signal case $\gamma = 2$ and a weak signal case $\gamma = 1$. We vary the number of observations $n \in \{50, 100, 200\}$, and we use a GP to model the CATE.

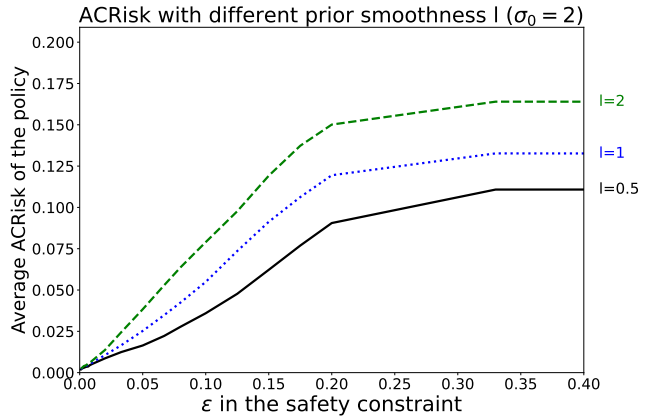
With covariate overlap. In the case with covariate overlap, there is no need for extrapolation. Therefore, we use a weak prior for the GP and specify the mean function $m(x) = 0$, the kernel function as a Matern kernel with $\sigma_0 = 4, l = 0.5$. We show how the average ACRisk and the value changes as a function of the safety constraint ϵ under different sample size and signal strength in Figure S8.

As shown in Figure S8, under all settings, the average ACRisk increases as the safety constraint ϵ increases. Given a fixed value of ϵ , a larger sample size and stronger signal lead to a lower ACRisk. Similar to the results in the main text, we find a regularization effect of the safety constraint, where under an appropriate value of the safety constraint, the average value of the learned policy is greater than that of the policy that maximizes the posterior expected utility without any safety constraint.

Without covariate overlap When there is no covariate overlap, the CATE must be extrapolated. We fix the sample size to 200 and the signal strength $\gamma = 2$ and investigate the average Value and ACRisk for learned policies with different priors. Figure S9 and Figure S10 shows the average Value and ACRisk of the learned policy as a function of the safety constraint ϵ under different prior smoothness and prior strength. We find that with a smoother or stronger prior, the learned policy leads to a greater average ACRisk as it extrapolates more aggressively.

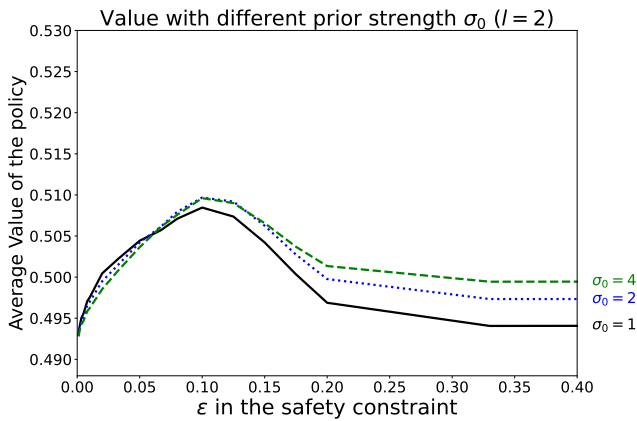


(a) Average Value

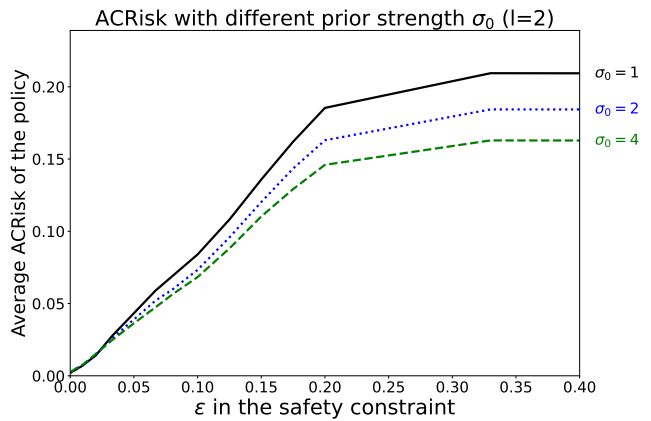


(b) Average ACRisk

Figure S9: Average Value and ACRisk for learned policies using data without covariate overlap, varying the safety constraint and prior smoothness for the CATE.



(a) Average Value

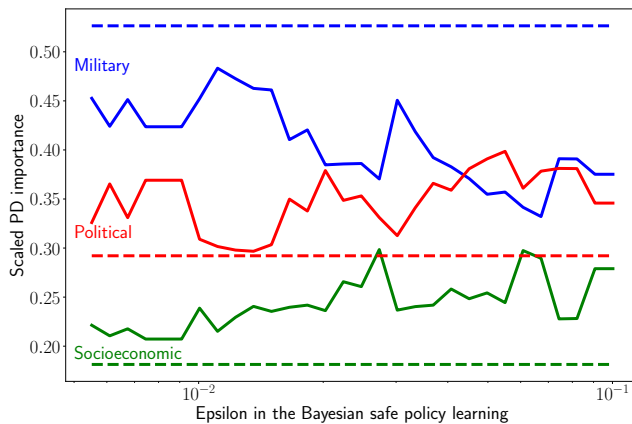


(b) Average ACRisk

Figure S10: Average Value and ACRisk for learned policies using data without covariate overlap, varying the safety constraint and prior strength for the CATE.

S6 Additional application results

S6.1 Scaled PD importance of level-3 scores



(a) Regional civic society as outcome

S6.2 Sensitivity analysis for prior hyperparameters

In the main text, we use a GP to estimate the CATE, relying on the GP prior for extrapolation. Here, we present a sensitivity analysis for the smoothness of the GP prior, which determines the degree of extrapolation. Other than the original setup where $l = 1$, we also consider the setups with $l = 0.5$ (less extrapolation on the CATE), $l = 2$ (more extrapolation on the CATE).

In Figure S12, we plot the partial dependence of the output security score as a function of the input level-3 score, under learned policies with different values of the prior smoothness parameter l . We use the regional safety as the outcome for policy learning, and set the safety parameter $\epsilon = 0.1$. As shown in Figure S12, with greater values of the prior smoothness parameter l for extrapolation, the obtained policies tend to systematically increase the output security score. This is consistent to the conclusion of Dell and Querubin (2018): airstrikes increased the communist insurgency activities and decreases regional safety. Specifically, the change of the partial dependence is larger when $l = 2$, which corresponds to a stronger smoothness prior and more extrapolation. When $l = 0.5$, there is less extrapolation and the change of the partial dependence is smaller.

We further plot the relative partial dependence importance of each level-3 scores as a function of the safety constraint ϵ , varying the prior smoothness parameter l . In Figure S12, under all the prior smoothness parameter, the learned policy downweights the military sub-model scores and upweights the socioeconomic sub-model scores.

S7 Optimization for Monotonic Decision Tables

In this section, we develop an optimization algorithm applicable to monotonic decision tables where the output of a decision table is non-decreasing in each input dimension.

S7.1 Problem definition

We define the *monotonic decision table* as below:

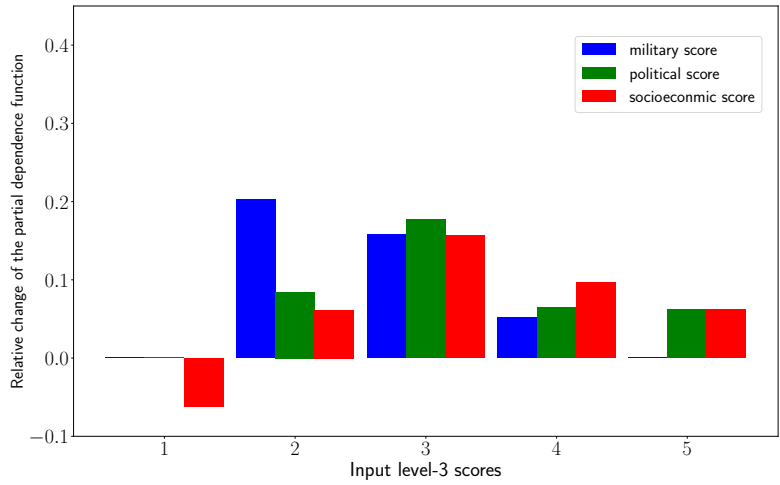
Definition S1 (Monotonic decision tables). Suppose $\mathcal{X}_1, \mathcal{X}_2, \dots, \mathcal{X}_p, \mathcal{Y}$ are finite totally ordered sets, T is a function that maps $x \in \mathcal{X} = \mathcal{X}_1 \times \mathcal{X}_2 \times \dots \times \mathcal{X}_p$ to \mathcal{Y} . Then, T is a monotonic decision table if and only if the following condition holds,

$$\forall x = \{x_i\}_{i=1}^p, x' = \{x'_i\}_{i=1}^p \in \mathcal{X} \text{ where } x_i \leq x'_i \text{ for } 1 \leq i \leq p, T(x_1, \dots, x_p) \leq T(x'_1, \dots, x'_p)$$

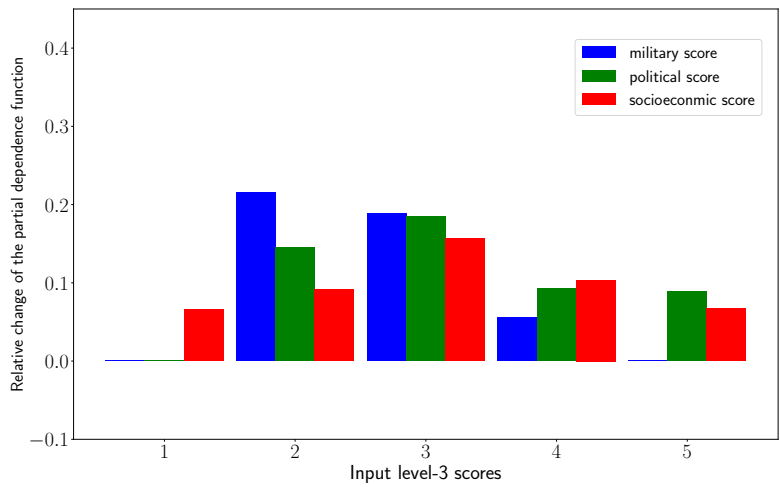
We consider the following general optimization problem over monotonic decision tables.

Definition S2 (Optimization with monotonic decision tables). Suppose f, g are functions that map a monotonic decision table T into a real-valued output. We consider the problem of finding an optimal monotonic decision table T_{opt} as defined below:

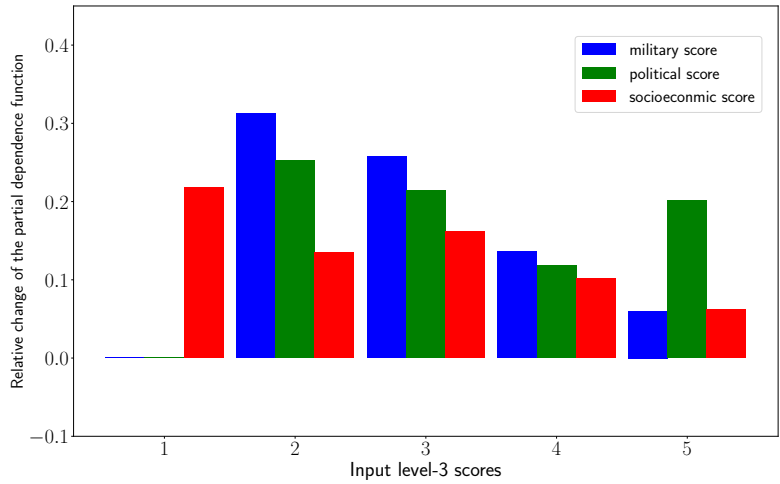
$$T_{opt} := \underset{T}{\operatorname{argmin}} f(T) \text{ subject to } g(T) \geq 0 \tag{S8}$$



(a) $l = 0.5$



(b) $l = 1$



(c) $l = 2$

Figure S12: The relative change of the PD function from the baseline policy to the learned policy for $\epsilon = 0.1$. Each block corresponds to the different input of the PD function, and different colors corresponds to different level-3 scores.

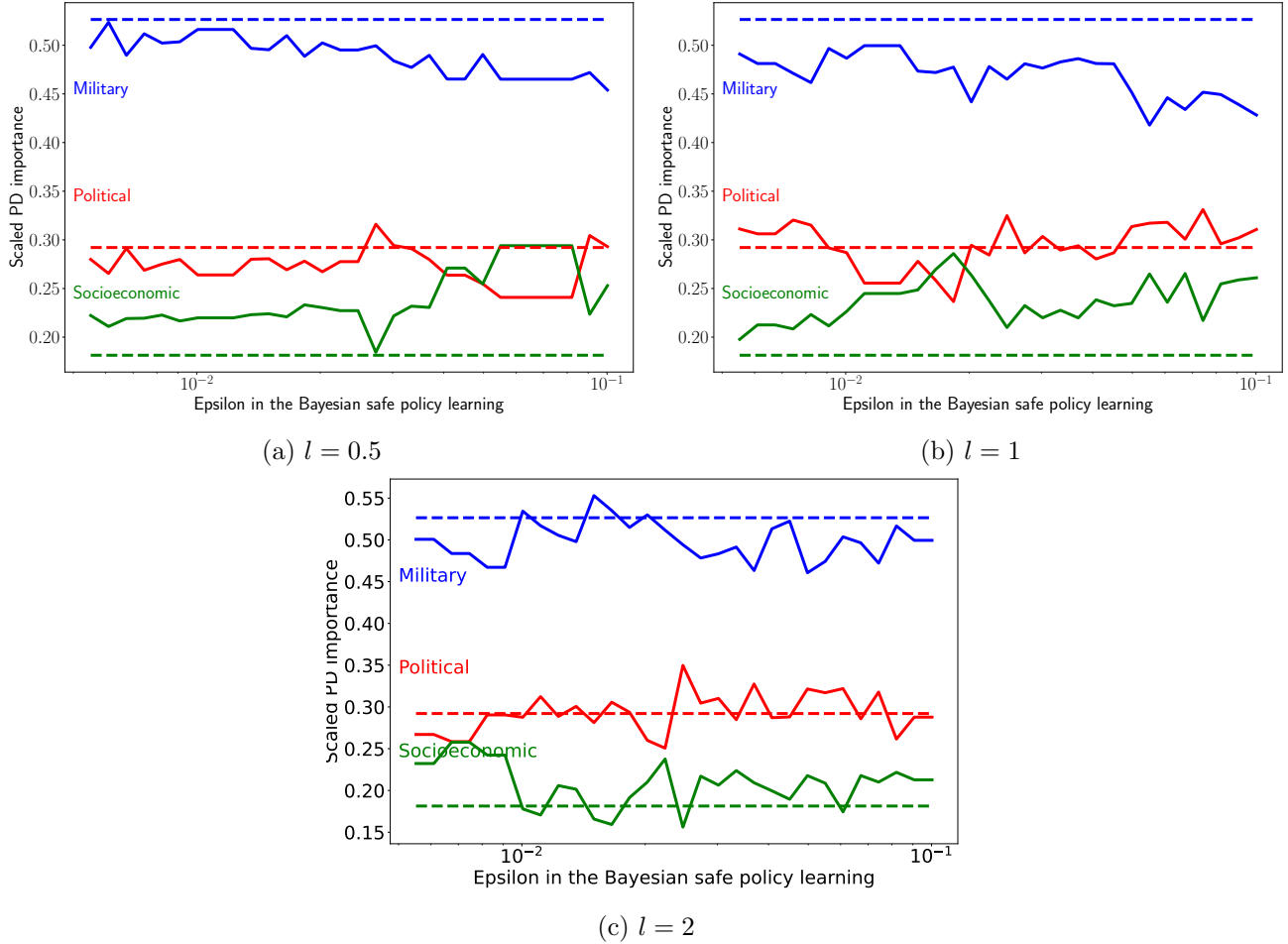


Figure S13: The scaled Partial Dependence (PD) importance of level-3 scores of the learned policy with regional safety outcomes, as a function of the ϵ . The solid line corresponds to the learned policy, and the dashed line indicates the baseline policy. Lines with different colors shows the PD importance of different level-3 scores.

In general, optimization over monotonic decision tables with the form given in Equation (S8) is difficult to solve. Although one could enumerate all possible monotonic decision tables and their corresponding $f(T), g(T)$, the number of enumerations is equal to $\mathcal{Y}^{|\mathcal{X}|} = \mathcal{Y}^{|\mathcal{X}_1| \times |\mathcal{X}_2| \times \dots \times |\mathcal{X}_p|}$, which grows exponentially as the size of the decision table increases. In our application, we wish to simultaneously learn one two-way decision table and one three-way decision table, yielding a total of $5^{25} \times 5^{125} = 5^{150}$ enumerations. We would like to avoid enumerating these many possibilities.

Therefore, we use a Markov chain Monte Carlo (MCMC)-based stochastic algorithm for optimizing over monotonic decision tables by adopting ideas from the graph theory. Specifically, we represent a monotonic decision tables as an equivalent directed acyclic graph (DAG) where the directed edges indicates the monotonicity conditions, and optimize over monotonic decision tables by sampling the DAGs using an MCMC algorithm.

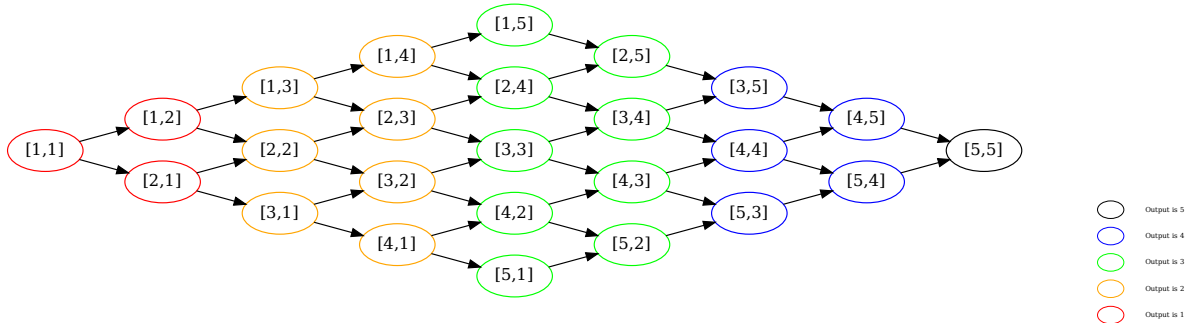


Figure S14: The DAG representation of the original 2-way decision table in the HES. Each vertex corresponds to an input of the 2-way table, and directed edges indicate the relative order the corresponding output should satisfy based on the monotonicity constraint. The color of the nodes indicate the output of the 2-way decision table in the original HES.

S7.2 Graph representation for monotonic decision tables

Monotonic decision tables can be equivalently represented as directed acyclic graphs (DAGs). We represent different inputs of decision tables as vertices of the DAG, and the monotonicity constraint on the decision table as directed edges in the graph. For example, Figure S14 shows the graph representation for the original two-way decision tables in the HES (Figure S1). The two-way decision table has $5 \times 5 = 25$ different inputs, which corresponds to the 25 vertices in the graph. The edges in the DAG indicate the monotonicity constraint that the output should satisfy according to the decision table. For example, in Figure S14, there is a directed edge from vertex $[1, 1]$ to vertex $[1, 2]$, which means that the output of the decision table for input $[1, 1]$ should be no greater than the output for input $[1, 2]$.

With this representation, finding a decision table from \mathcal{X} to \mathcal{Y} is equivalent to finding a graph partition that separate the DAG into $|\mathcal{Y}|$ areas where vertices in the same area have the same output scores. A monotonicity constraint on the decision table is equivalently translated to an *acyclic* constraint on the partition, where we forbid any directed edges from a node with larger output to a node with a smaller outcome (Herrmann et al., 2017, 2019).

Figure S14 shows the graph partition corresponding to the original two-way decision table in the HES, where the color of a node indicates the partition. This satisfies the monotonicity constraint. In contrast, Figure S15 shows a different partition that does not satisfy the monotonicity constraint. There is a directed edge from $[3, 1]$ to $[3, 2]$, but the output for $[3, 1]$ is larger than the output for $[3, 2]$.

S7.3 Optimization by sampling partitions of the DAGs

We optimize over monotonic decision tables by finding optimal acyclic partitions of the corresponding DAGs. We propose an MCMC-based stochastic algorithm for sampling acyclic partitions of the DAGs and optimize over it. To do this, we first sample a *topological sort* of a DAG (Karzanov and Khachiyan, 1990) and then segment the topological sort into $|\mathcal{Y}|$ pieces to obtain a partition of the DAG.

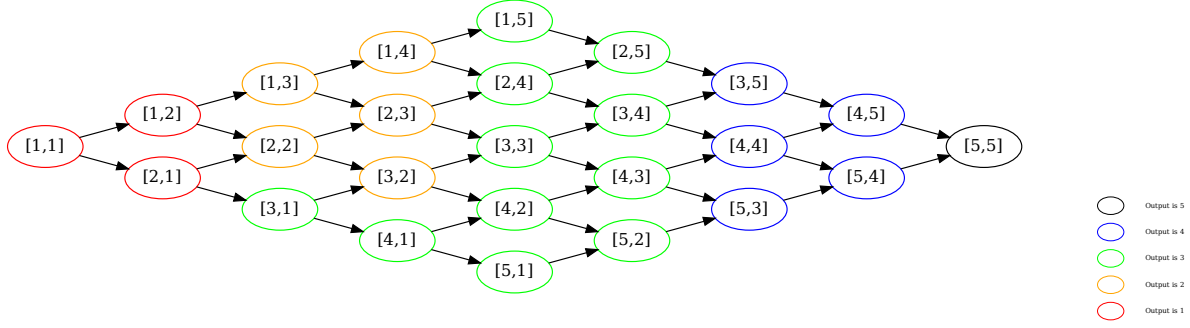


Figure S15: An example of partition for a decision table that does not satisfy the monotonicity constraint. There is a directed edge from $[3, 1]$ to $[3, 2]$, but the output for $[3, 1]$ is larger than the output for $[3, 2]$.

Algorithm 1: Stochastic Optimization Algorithm for Monotonic Decision Tables

Data: DAG \mathcal{G} that contains all the potential inputs of the decision table and relations from monotonicity constraints; Markov chain \mathcal{M} that generates an acyclic partial partition of \mathcal{G} with a uniform stationary distribution; Initial monotonic decision table T_0 and corresponding state S_0 of \mathcal{M} .

```

1 for  $0 \leq r \leq R$  do
2    $S_{r0} \leftarrow S_r$ 
3    $T_{r0} \leftarrow T_r$ 
4   for  $1 \leq k \leq K$  do
5      $S_{rk} \leftarrow \mathcal{M}(S_{r(k-1)})$ 
6      $T_{rk} \leftarrow$  Decision table that corresponds to  $S_{rk}$ 
7   end for
8    $S_{r+1} \leftarrow \arg \min_{T \in \{T_{r0}, T_{r1}, \dots, T_{rK}\}} f(T)$  subject to  $g(T) \geq 0$ 
9    $T_{r+1} \leftarrow$  Decision table corresponds to  $S_{r+1}$ ;
10 end for
11 Return  $T_{R+1}$ 

```

Definition S3. (Topological sort on DAG) A topological sort of a directed acyclic graph (DAG) is a linear ordering of its vertices such that for every directed edge uv from vertex u to vertex v , u comes before v in the ordering.

We take advantage of the fact that any segmentation of a topological sort corresponds to an acyclic partition and produces a decision table satisfying the monotonicity constraint. Conversely, for any decision table satisfying the monotonicity constraint, there will be a corresponding topological sort and segmentation that produces the decision table. We use the MCMC algorithm of [Karzanov and Khachiyan \(1990\)](#) to sample a topological sort from the DAG and a random walk to sample segmentations of the topological sorts. This gives us a Markov chain that generates random acyclic partitions. Finally, we use a *short-burst* algorithm to use the MCMC sampling algorithm for optimization ([Cannon et al., 2023](#)). Algorithm 1 formally describes our optimization procedure.

In the application, we run the above algorithm 2000 times to obtain 2000 corresponding decision

tables. Then we choose the one that achieves the highest posterior expected value.

References

- Ben-Michael, E., Greiner, D. J., Imai, K., and Jiang, Z. (2021). Safe policy learning through extrapolation: Application to pre-trial risk assessment. *arXiv preprint arXiv:2109.11679*.
- Branson, Z., Rischard, M., Bornn, L., and Miratrix, L. W. (2019). A nonparametric bayesian methodology for regression discontinuity designs. *Journal of Statistical Planning and Inference*, 202:14–30.
- Cannon, S., Goldbloom-Helzner, A., Gupta, V., Matthews, J., and Suwal, B. (2023). Voting rights, markov chains, and optimization by short bursts. *Methodology and Computing in Applied Probability*, 25(1):36.
- Chipman, H. A., George, E. I., and McCulloch, R. E. (2010). Bart: Bayesian additive regression trees.
- Dell, M. and Querubin, P. (2018). Nation building through foreign intervention: Evidence from discontinuities in military strategies. *The Quarterly Journal of Economics*, 133(2):701–764.
- Hahn, P. R., Murray, J. S., and Carvalho, C. M. (2020). Bayesian regression tree models for causal inference: Regularization, confounding, and heterogeneous effects (with discussion). *Bayesian Analysis*, 15(3):965–1056.
- Herrmann, J., Kho, J., Uçar, B., Kaya, K., and Çatalyürek, Ü. V. (2017). Acyclic partitioning of large directed acyclic graphs. In *2017 17th IEEE/ACM international symposium on cluster, cloud and grid computing (CCGRID)*, pages 371–380. IEEE.
- Herrmann, J., Özkaya, M. Y., Uçar, B., Kaya, K., and Çatalyürek, U. V. (2019). Multilevel algorithms for acyclic partitioning of directed acyclic graphs. *SIAM Journal on Scientific Computing*, 41(4):A2117–A2145.
- Karzanov, A. and Khachiyan, L. (1990). *On the conductance of order Markov chains*. Rutgers University, Department of Computer Science, Laboratory for Computer
- Rasmussen, C. E. and Williams, C. K. I. (2006). Gaussian processes for machine learning. The MIT Press.
- Taddy, M., Gardner, M., Chen, L., and Draper, D. (2016). A nonparametric bayesian analysis of heterogenous treatment effects in digital experimentation. *Journal of Business & Economic Statistics*, 34(4):661–672.